Universidade do Minho
Escola de Engenharia

Maria João Caetano da Costa

Engineering phages towards *Pseudomonas aeruginosa* detection and control

October 2022

Engineering phages towards *Pseudomonas aeruginosa* detection and control

Maria João Caetano da Costa

UMinho | 2022

Universidade do Minho
Escola de Engenharia

Maria João Caetano da Costa

Engineering phages towards *Pseudomonas aeruginosa* detection and control

Master's Thesis
Master's degree in Biotechnology

Work supervised by
Doctor Diana Priscila Penso Pires
Doctor Sílvio Roberto Branco dos Santos

October 2022

Nome: Maria João Caetano da Costa
Endereço eletrónico: pg42895@uminho.pt
Título da dissertação: Engineering phages towards *Pseudomonas aeruginosa* detection and control

Orientadores:
Doutora Diana Priscila Penso Pires
Doutor Sílvio Roberto Branco dos Santos

Ano de conclusão: 2022
Mestrado em Biotecnologia

DIREITOS DE AUTOR E CONDIÇÕES DE UTILIZAÇÃO DO TRABALHO POR TERCEIROS

AGRADECIMENTOS

No final deste percurso tão intenso e desafiante, não podia deixar de expressar o meu agradecimento a todos os que me acompanharam e apoiaram durante toda esta etapa profissional e pessoal que chega agora ao fim.

Primeiramente gostaria de agradecer à Doutora Diana Priscila Pires e Doutor Sílvio Santos, orientadores da minha dissertação de mestrado, por me receberem tão bem neste projeto. Sou uma privilegiada por toda a experiência e formação que me proporcionaram. Agradeço a presença constante, dedicação, paciência, confiança e por serem incansáveis neste trabalho. Todo o vosso apoio, profissionalismo, excelência e rigor científico alargaram os meus horizontes ao longo desta jornada e tornaram-me preparada para novos desafios.

Ao grupo do LPhage, agradeço por me terem recebido tão bem neste laboratório. Obrigada pela vossa companhia, disponibilidade e transmissão de conhecimento sempre de forma tão atenciosa. Foi um prazer trabalhar convosco e sem vocês não seria o mesmo. Toda a vossa boa disposição, carinho e ajuda contribuíram para que tudo isto se tornasse possível.

Obrigada aos amigos incríveis que tenho. Agradeço terem cruzado o meu caminho, desde Marco de Canaveses, Vila Real ou Braga, pela vossa amizade incondicional, companheirismo, motivação e boa disposição capazes de transformar uma lágrima num sorriso. Tornaram este percurso mais fácil!! Ao Bruno, obrigada pelo apoio incansável nos momentos mais difíceis, por teres sempre uma palavra de conforto, pelo carinho e por toda a cumplicidade. Obrigada por estares sempre presente, acreditares e me fazeres acreditar que tudo isto seria possível.

Por último, quero agradecer aos meus pais por tornarem todo este percurso possível, apoiarem em todos os momentos e estarem sempre presentes. O maior agradecimento será sempre para vós que me permitem, todos os dias, lutar pelos meus objetivos. Como não podia deixar de ser, quero também agradecer aos meus irmãos, Flávia e Marco! Apesar de me roubarem os panados e teimarem em contrariar comigo, sei que torcem por mim. Aos meus avós, que sempre tiveram fé nas minhas conquistas, um abracinho especial.

Este trabalho foi financiado por fundos nacionais através da FCT – Fundação para a Ciência e a Tecnologia, I.P., no âmbito do projeto "PhageShaper – uma plataforma eficiente para editar fagos de *P. aeruginosa* para o controlo de doenças infecciosas" com a referência EXPL/EMD-EMD/1142/2021.

Obrigado!

FCT Fundação para a Ciência e a Tecnologia
MINISTÉRIO DA CIÊNCIA, TECNOLOGIA E ENSINO SUPERIOR

STATEMENT OF INTEGRITY

I hereby declare having conducted this academic work with integrity. I confirm that I have not used plagiarism or any form of undue use of information or falsification of results along the process leading to its elaboration.

I further declare that I have fully acknowledged the Code of Ethical Conduct of the University of Minho.

SUMÁRIO

A *Pseudomonas aeruginosa* é uma bactéria Gram-negativa que prospera numa variedade de ambientes. Esta bactéria patogénica é um dos microrganismos mais frequentemente isolados do trato respiratório de pacientes em estado crítico e imunocomprometido. Para além disso, o seu frequente envolvimento numa ampla gama de doenças e a sua baixa suscetibilidade a uma ampla gama de antibióticos, torna *P. aeruginosa* um sério desafio terapêutico, que muitas vezes resulta em internamentos prolongados, aumento dos custos médicos e altas taxas de mortalidade.

Face a isto, o desenvolvimento de abordagens alternativas ao uso destes antimicrobianos é de extrema importância e os bacteriófagos têm um elevado potencial no controlo de doenças bacterianas, mas geralmente exibem um espetro de ação limitado. Através da utilização de ferramentas de engenharia de fagos, é possível produzir fagos quiméricos com características desejáveis de forma a melhorar a deteção e/ou controlo de estirpes bacterianas num contexto clínico. Além disso, os fagos modificados podem codificar vários genes repórter, substituindo assim os métodos de cultura convencionais.

O objetivo deste projeto assenta na engenharia do genoma de fagos de *P. aeruginosa* para melhorar as suas funcionalidades, assim como aumentar o seu espetro de ação para uma ampla gama de bactérias hospedeiras e obter uma ferramenta promissora para o diagnóstico e tratamento de pacientes com infeções resistentes a antibióticos. O primeiro passo deste trabalho consistiu em avaliar o potencial de um fago repórter previamente construído, contendo o gene da NanoLuc luciferase (PE3Δgp1–gp12:Nluc) para detetar células de *P. aeruginosa*. O limite de deteção deste fago repórter variou entre 620 e 9000 UFC/mL em apenas 7 h, sendo o limite de deteção mais baixo alcançado para a estirpe hospedeira do fago. Posto isto, este sistema de deteção baseado em fago constitui uma alternativa promissora aos métodos de cultura, já que permite um diagnóstico mais rápido.

A fim de aumentar o espetro lítico deste fago, foi realizada uma análise genómica para os fagos de *Pseudomonas* phiIBB-PAA2 e vB_PaeP_PE3. Desta forma, foram identificadas e selecionadas potenciais Tail Fiber Proteins (TFPs). Sete proteínas codificadas nos genomas dos fagos foram selecionadas e de seguida clonadas, expressas e purificadas, mas apenas uma (pGFP_A2gp55) foi capaz de se ligar a células de *P. aeruginosa* PAO1. Com base nestes ensaios, foi usada uma ferramenta de engenharia de fagos baseada em levedura para inserir com sucesso a TFP funcional (*gp*55) do fago A2 no genoma do fago PE3Δgp1–gp12:Nluc. Ainda assim, este método não permitiu aumentar o espetro de hospedeiros do fago.

Palavras-chave: *Pseudomonas aeruginosa*, resistência antibiótica, bacteriófagos, engenharia de fagos, fagos quiméricos, deteção de patógenos, controlo de patógenos, limite de deteção.

ABSTRACT

Pseudomonas aeruginosa is a Gram-negative bacterium that thrives in a variety of environments. This bacterial pathogen is one of the most common microrganims frequently isolated from the respiratory tract of critically ill and immunocompromised pacients. In addition, its frequent involvement in a wide range of illnesses and its low susceptibility to a wide range of antibiotics, makes *P. aeruginosa* a serious therapeutic challenge, which often results in prolonged hospital stays, increased medical costs, and high mortality rates.

Given this, the development of alternative approaches to the use of these antimicrobials is extremely important and bacteriophages have a tremendous potential against bacterial diseases but they usually exhibit a limited host range. Taking advantage of phage-engineering tools, it is possible to assemble chimeric phages with desirable features in order to improve the detection and/or control bacterial strains in clinical settings. In addition, engineered phages can encode numerous reporter genes, therefore replacing the conventional culture methods.

The aim of this project relies on engineering the genome of *P. aeruginosa* phages to improve its performance by expanding their host range, in order to get a promising tool for the diagnosis and treatment of patients with antibiotic-resistant infections. This research's initial step was to evaluate how well a previously built reporter phage (PE3gp1-gp12:Nluc) could identify *P. aeruginosa* cells. The lowest detection limit for the phage host strain *P. aeruginosa* PAO1 was reached by this reporter phage, whose detection limit ranged from 620 to 9000 CFU/mL in only 7 hours. Nevertheless, because it enables quicker diagnosis, this phage-based detection technology is a possible replacement for culture approaches. To increase the host range of this phage, a genomic analysis was performed for the *Pseudomonas* phages phiIBB-PAA2 and vB_PaeP_PE3. This method allowed for the identification and selection of prospective Tail Fiber Proteins (TFPs). Seven selected proteins encoded in phage genomes were then cloned, expressed and purified, but only one (pGFP_A2gp55) was capable of binding to *P. aeruginosa* PAO1 cells. Based on these assays, the yeast-based phage-engineering tool was used to successfully insert the functional TFP (*gp*55) from A2 phage on PE3Δgp1–gp12:Nluc phage genome. However, this approach was unable to broaden the range of phage hosts.

Keywords: *Pseudomonas aeruginosa*, antibiotic resistance, bacteriophages, phage-engineering, chimeric phages, pathogen detection, pathogen control, limit of detection.

TABLE OF CONTENTS

LIST OF ABBREVIATIONS

BIMs	Bacteriophage Insensitive Mutants
BLASTP	Basic Local Alignment Search Tool Protein
BRED	Bacteriophage Recombineering of Electroporated DNA
CDSs	Coding Sequences
CF	Cystic Fibrosis
CRISPR	Clustered Regularly Interspaced Short Palindromic Repeats
CSM-Leu	Complete Supplement Mixture - Leucine
DNA	Deoxyribonucleic acid
ELISA	Enzyme-linked immunosorbent assay
EPS	Extracellular Polymeric Substances
FISH	Fluorescent In Situ Hybridization
GFP	Green Fluorescent Protein
LB	Luria Broth
LPS	Lipopolysaccharides
MALDI-TOF MS	Matrix-assisted laser desorption/ionization time of flight mass spectrometry
MCS	Multiple Cloning Site
MTA-LB	Molten Top Agar – Luria Broth
NCBI	National Center for Biotechnology Information
Nluc	Nanoluc luciferase
PCR	Polymerase Chain Reaction
QS	Quorum Sensing
RBPs	Receptor-Binding Proteins
real-time qPCR	real-time quantitative PCR
RLUs	Relative Light Units
RM	Restriction Modification
RNA	Ribonucleic acid
RT-PCR	Reverse Transcription PCR
SD-Leu	Synthetic Defined (medium)– Leucine
SM Buffer	Saline Magnesium Buffer
SOC	Super Optimal broth with Catabolite repression

TFPs	Tail Fiber Proteins
T3SS	Type III Secretion System
WHO	World Health Organization
YAC	Yeast Artificial Chromosome
YPD	Yeast Extract-Petone Dextrose

LIST OF FIGURES

Chapter 1

Chapter 2

Chapter 3

LIST OF TABLES

Chapter 2

Chapter 3

Supplementary material

Chapter 1

INTRODUCTION

1. INTRODUCTION

1.1. Overview of *Pseudomonas aeruginosa* clinical impact

Pseudomonas aeruginosa is an ubiquitous Gram-negative bacterium belonging to the *Pseudomonadaceae* family that is capable of surviving in a wide range of environments (Pachori et al., 2019; Silby et al., 2011). This opportunistic bacterium can be found in water, soil and plants, infecting many different organisms, such as yeasts, plants, nematodes, insects and mammals (Pachori et al., 2019; Pereira et al., 2014). In humans, *P. aeruginosa* is one of the most frequent pathogens isolated from the respiratory tract of critically ill and immunocompromised patients and is considered the main cause of morbidity and mortality in patients with ventilator-associated pneumonia and cystic fibrosis (CF). *P. aeruginosa* is also frequently involved in many other infections, including catheter-associated infections, burn wound infections, bloodstream infections, urinary tract infections, and surgical site infections, thus constituting a real and high concern in hospital settings. Indeed, this pathogen is a major cause of nosocomial bacteraemia, with a very high (>30 %) associated mortality rate (Bassetti et al., 2018; Juan et al., 2017; Nguyen et al., 2018; Pachori et al., 2019; Pereira et al., 2014). According to the Centers for Disease Control and Prevention, (2019), in 2017 there were an estimated 32.600 cases of infections caused by *P. aeruginosa* in hospitalized patients and approximately 2.700 deaths in US, corresponding to $ 767M of health care costs.

P. aeruginosa possesses an arsenal of several virulence factors to evade host cell defences. These virulence mechanisms include adhesins, proteases, phenazines, pyocyanin, exotoxins of the type III secretion system (T3SS), flagella or lipopolysaccharides (LPS). These virulence factors have specific roles to counteract host defences. Adhesins, for instance, participate in the initial stage of infection, allowing bacteria to adhere to host cells. Proteases, mainly alkaline protease and elastase, degrade elastin, which represents 28 % of the lung tissue. Phenazins increase intracellular oxidative stress, inhibiting mitochondrial activity and cell proliferation in neutrophils and macrophages. T3SS promotes apoptosis of eukaryotic cells and the spread of the disease through the lung (Passador et al., 1993; Pereira et al., 2014; Strateva & Mitov, 2011). Many of the *P. aeruginosa* virulence factors are regulated by quorum-sensing (QS), a cell-cell communicating mechanism that controls gene expression based in fluctuations on cell density. Two distinct QS systems are known in *P. aeruginosa*: las and rhl (Reuter et al., 2016; Strateva & Mitov, 2011). Besides the virulence factors described above, *P. aeruginosa* also has an innate ability to form biofilms, which can be defined as aggregates of bacteria encased in a self-

produced matrix of extracellular polymeric substances (EPS) that confers protection to the bacterial cells. Therefore, these complex structures are very difficult or even impossible to eradicate with antibiotic treatment (Ciofu & Tolker-nielsen, 2019; Moradali et al., 2017), being a huge challenge in clinical settings.

P. aeruginosa resistance may be expressed by three different forms (**Figure 1**) to a wide range of antibiotics, such as β-lactams, aminoglycosides, quinolones and polymyxins (Bassetti et al., 2018; Heinz et al., 2019; Klockgether et al., 2011; Pachori et al., 2019).

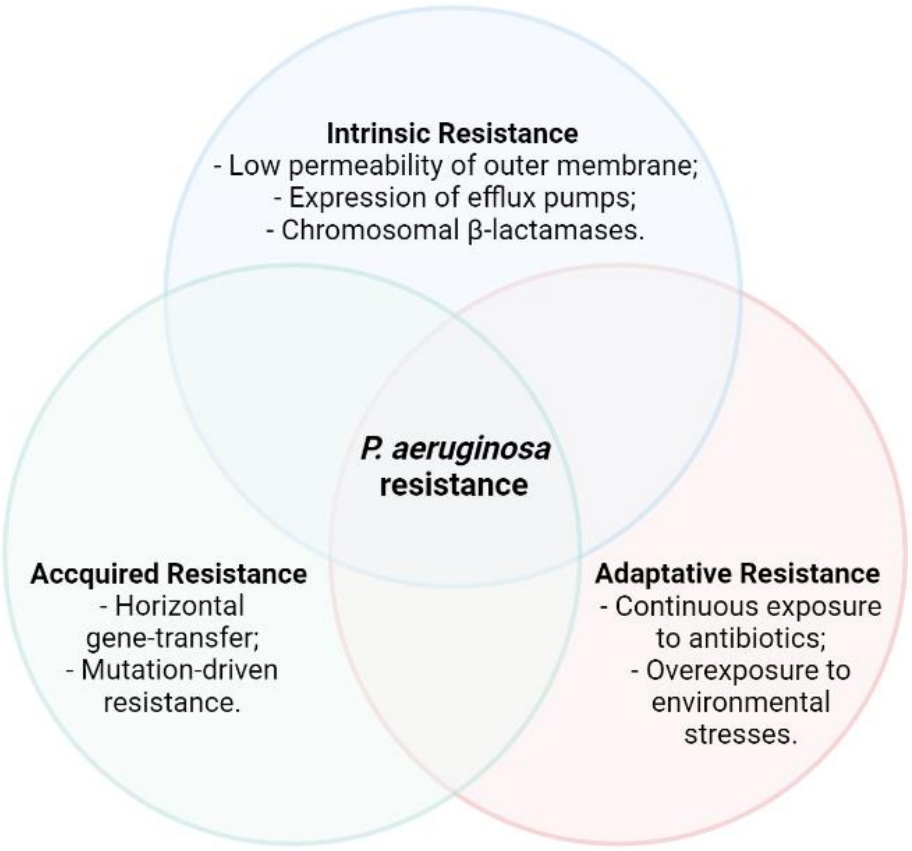

Figure 1 - *Pseudomonas aeruginosa* resistance mechanisms.

The intrinsic resistance of *P. aeruginosa* includes low permeability of the outer membrane, expression of efflux pumps that expel antibiotics out of the cell, and the production of antibiotic inactivating enzymes (Breidenstein et al., 2011; Ghysels et al., 2008; Pachori et al., 2019). The acquired resistance of *P. aeruginosa* can be achieved by horizontal transfer of resistance genes or mutational changes (Breidenstein et al., 2011; Pachori et al., 2019). Adaptive resistance is inducible and dependent

on the continued presence of an antibiotic or another environmental stimulus. Several triggering factors are now qualified to induce this type of resistance, including antibiotics, biocides, polyamines, anaerobiosis, cations, pH and carbon sources, as well as biofilm formation. These factors modulate the expression of many genes, leading to effects on the efflux pumps, cell envelope, and enzymes. An important feature of adaptive resistance is that, once the inducing factor or condition is removed, the organism reverts to wild-type susceptibility. Adaptive resistance can also have long-term consequences. If cells are not completely eradicated, as soon as the treatment stops, growth can be observed (Breidenstein et al., 2011). This is of particular concern in clinical environments where *P. aeruginosa* grows as a biofilm (Breidenstein et al., 2011).

The overuse and misuse of antibiotics is a growing public health concern, which can result in negative side effects and the development of drug-resistant bacterial strains (Takahashi & Tatsuma, 2014). According to Bassetti et al. (2018), infections related to *Pseudomonas spp*. were reported in 60 % of his studies and overall, mortality ranged from 33 to 71 % in patients with carbapenem-resistant *Pseudomonas* infections. In addition to mortality, resistance is also associated with increased healthcare costs (Bassetti et al., 2018). Moreover the development of new antibiotics is currently very limited and time-consuming (Pang et al., 2019).

In 2017, the World Health Organization (WHO) published a global priority list of antibiotic-resistant bacteria that urgently require the development of new antibiotics (World Health Organization, 2017). The most critical group includes multi-resistant bacteria that pose a specific threat in hospitals, nursing homes and among patients whose care requires devices such as ventilators and blood catheters. This group includes *Acinetobacter baumannii*, *P. aeruginosa* and several *Enterobacteriaceae*. Thus, the discovery and development of alternative therapeutic strategies to control *P. aeruginosa* infections is urgent (Breidenstein et al., 2011; Chatterjee et al., 2016; Pachori et al., 2019). These new therapeutic strategies can act alone or in combination with conventional therapies, and may include QS inhibitors, iron chelation molecules, vaccine strategy, nanoparticles, antimicrobial peptides, electrochemical scaffolding and phage therapy (Pang et al., 2019).

1.2. Diagnostic methods for detection of *Pseudomonas aeruginosa* in clinical settings

At incredibly low quantities, *Pseudomonas aeruginosa* can cause illnesses; just 10–100 bacilli can colonize the intestine of extremely ill or immunocompromised patients, which can result in persistent and long-term infections. Long turnaround times for diagnoses can worsen patient outcomes and raise

hospital costs (Tang et al., 2017). In addition to the development of new therapies to treat *P. aeruginosa* infections, it is also urgent the development of fast and accurate tools to detect *P. aeruginosa* in clinical settings, replacing the conventional methods that are usually laborious and time-consuming.

The biological characteristics of the bacterium under specific culture conditions or the activities of bacterial molecules like oxidase, acetamidase, arginine dihydrolase, and pyocyanin are the basis for conventional *Pseudomonas aeruginosa* detection methods (Tang et al., 2017). Bacteria are most frequently detected by culture methods using selective and non-selective media. *P. aeruginosa* is easily grown in different media and these media play an important role in their detection. In blood agar, a non-selective medium, *P. aeruginosa* is sometimes overgrown by the commensal flora (Xu et al., 2004). Gram-negative selective media, such as McConkey agar, make the discrimination of *P. aeruginosa* from other respiratory pathogens and native flora more convenient. Selective media such as *P. aeruginosa* isolation agar or cetrimide agar were especially developed for the culture of *P. aeruginosa* (Tramper-stranders et al., 2005; Xu et al., 2004). However, these old procedures have some significant limitations and frequently require more than 48 h for early results (Tramper-stranders et al., 2005).

On the other hand, infection with *P. aeruginosa* can be proven both by the culture of the organism itself and by the detection of the immune response to the microorganism. The antibody test with ELISA (Enzyme-linked immunosorbent assay) demonstrated little or no interference from cross-reactive antibodies directed against other bacteria (Tramper-stranders et al., 2005). Chronic infection generally causes a high antibody response (Burns et al., 2001; Tramper-stranders et al., 2005).

The polymerase chain reaction (PCR) of samples has been used for the detection of *P. aeruginosa* in patients with CF at an early stage and has a high sensitivity for *P. aeruginosa*. Serological and molecular techniques are particularly useful for initial or intermittent colonization, because chronic colonization is usually easily confirmed by culture (Tramper-stranders et al., 2005). In order to discriminate between viable and non-viable cells, reverse transcription PCR (RT-PCR) has been created. Because these tests amplify RNA, a product of ongoing cellular and metabolic activities, only recently alive organisms may be identified (Anbu et al., 2017; Young et al., 2005). Due to higher false-positive results as compared to culture and other approaches, as well as technical difficulties and costs, RT-PCR-based detection methods are not frequently employed, raising questions about their efficacy. (Jones et al., 2020; Schmelcher & Loessner, 2014).

By adding fluorescent molecules to the reaction mixture, the real-time, fluorescence-based quantitative PCR (real-time qPCR) approach offers a quantitative detection through real-time monitoring

of PCR reactions and is one of the most popular nucleic acid-based molecular detection methods for pathogens at the moment. This technique allowed the detection of *P. aeruginosa* in CF patients more quickly. Real-Time fluorescence-based PCR was also a leading method for the detection of pathogens in respiratory tract infections and pneumonia, and it was a very sensitive, powerfully speedy, extensively applicable, and prospectively detectable instrument (Tang et al., 2017).

FISH (Fluorescent In Situ Hybridization) is another technique used for bacterial detection; however, the sensitivity, percentage of target strains that are detected with FISH compared to the culture is not very high, as the microscopic detection limit depends on samples of high bacterial density. In addition, the procedure is not simple and does not discriminate between dead and live cells (Hogardt et al., 2000; Tramper-stranders et al., 2005).

A novel kind of soft ionization mass spectrometry called matrix-assisted laser desorption/ionization time of flight mass spectrometry (MALDI-TOF MS) is used to map the protein spectrum of microbes. To obtain an identification, the mass spectrometry data of clinical microorganisms are compared with the common protein database of recognized bacteria. MALDI-TOF MS has becoming a fast and effective microbial identification method used in clinical diagnostics, environmental monitoring, and microbiological classification research due to its speed, accuracy, sensitivity, automation, and high throughput. This method has also been used by some researchers to identify *P. aeruginosa* (Tang et al., 2017).

These quick procedures, nevertheless, are hindered by the need for expensive equipment, time-consuming pre-enrichment steps, and challenging results handling and interpretation (MALDI-TOF MS) (Schmelcher & Loessner, 2014).

Various biorecognition components, including antibodies, enzymes, aptamers, and nucleic acids, have been used extensively in recent years and are essential for the detection of infections in a variety of complicated matrices. Antibodies against *P. aeruginosa* can appear months before a culture becomes positive, and are a useful parameter for monitoring infection in patients colonized with *P. aeruginosa*, as titres may vary with antimicrobial treatment but these compounds are laborious and expensive to produce, have high detection limits, and frequently exhibit cross-reactivity (Costa et al., 2022; Tramper-stranders et al., 2005). Bacteriophages are good candidates to replace traditional recognition molecules due to their interesting properties, including high specificity, sensitivity, stability, and ease of engineering (Costa et al., 2022). In addition, since they only multiply in viable cells, they can also discriminate between live and dead cells, are simple and affordable to produce, and exhibit high resistance to changes

in temperature and pH, chemical solvents, and proteases (Schmelcher & Loessner, 2014). These properties can improve the early detection of *P. aeruginosa* in clinical settings since aggressive antimicrobial therapy can prevent growth and detection of *P. aeruginosa* through culture methods. (Tramper-stranders et al., 2005).

1.3. Bacteriophages

1.3.1. Definition and infection cycles

About 100 years ago, Félix d'Hérelle discovered the viruses of bacteria - bacteriophages (phages). Their ability to predate bacteria quickly prompted its use to treat and prevent infectious diseases in humans and animals (Lin et al., 2017; Monteiro et al., 2019). Phages are simple, yet extremely diverse, biological entities that consist of DNA or RNA encased in a protein capsid.

As naturally occurring bacterial parasites, phages are unable to reproduce independently and are ultimately dependent on a bacterial host for survival (Lin et al., 2017). The infection begins with the adsorption of the phage to specific bacterial receptors located on the cell surface and this causes the genome of the phage to be ejected into the cell. The subsequent replication strategy defines the phage as strictly lytic or temperate (**Figure 2**) (Lin et al., 2017; Monteiro et al., 2019).

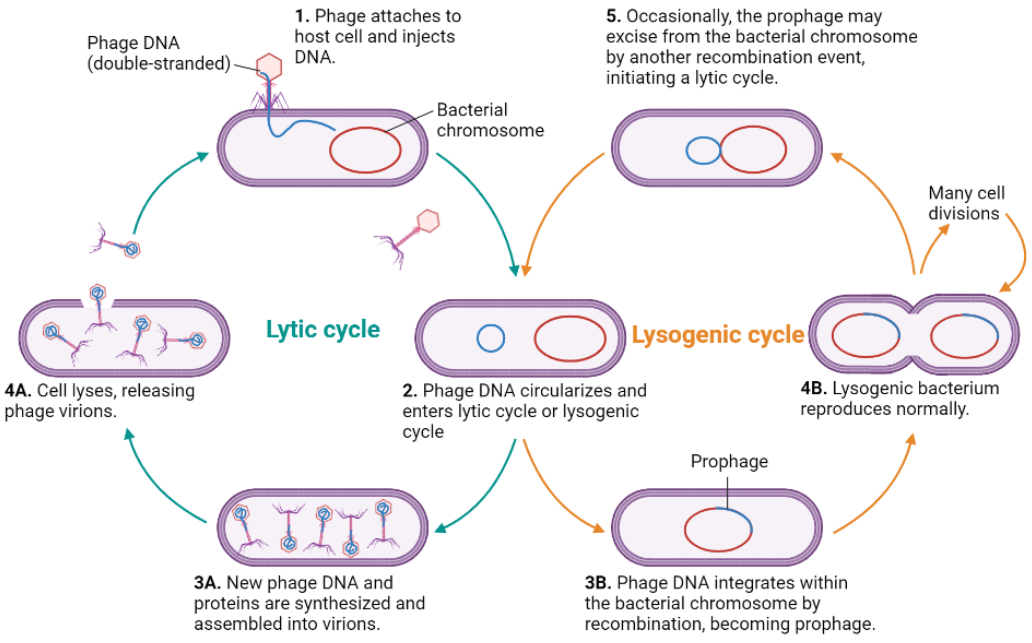

Figure 2 - Bacteriophage infection cycle. Adapted from Gaydos, (2018).

Strictly lytic or virulent phages always follow a lytic life cycle in which, immediately after the genome is ejected, the expression of the phage's early genes redirects the host's metabolism to phage DNA replication and protein synthesis. Viral proteins are then assembled, and the viral genome is packaged in capsids. At the end of the lytic cycle, the production of late phage proteins, such as holins and endolysins, leads to cell lysis and release of progeny phages that will be available to start a new cycle of infection (Drulis-kawa et al., 2012; Kortright et al., 2019; Monteiro et al., 2019).

Temperate phages can follow a lysogenic cycle in which they usually integrate their genome with the host chromosome, where they remain quiescent, as prophages. The prophage replicates with the bacterial chromosome and is subsequently transmitted by cell division to the daughter cells. This quiescent state can be maintained for long periods, unless the cell is exposed to an environmental stimulus that can cause the phage to be induced into a lytic cycle (Davies et al., 2016; Kortright et al., 2019; Lin et al., 2017; Monteiro et al., 2019).

In addition, phages can assume a pseudolysogenic cycle, in which the phage genome is transported in host cells without propagation (lytic cycle) or replication with the cell genome (lysogenic cycle). The non-integrated phage genome is inherited by only one of the emerging descendent cells. This phenomenon is apparently caused by unfavourable growth conditions for host cells, such as severe hunger, and ends when those conditions cease; the phage then restarts its development through the lytic or lysogenic life cycle (Lin et al., 2017; Monteiro et al., 2019).

1.3.2. Advantages and limitations of phages

In consequence of the global spread of antibiotic resistance, phages are becoming increasingly attractive as an alternative therapeutic approach against antibiotic-resistant bacterial infections (Pirnay et al., 2018).

Theoretically, there are no bacteria that cannot be lysed by at least one phage. One of the most important characteristics of phages is their high specificity, meaning that they have the ability to kill only the pathogen that they can recognize (Principi et al., 2019).This high specificity avoids the most important problem related to the administration of antibiotics, which is their influence on the entire microbiome with the elimination of potentially beneficial bacteria (Domingo-Calap & Delgado-Martínez, 2018; Loc-carrillo & Abedon, 2011). In addition to the high specificity, phages offer some other important advantages over antibiotics. One of them is that their isolation, typically from wastewater and sewage, is usually relatively easy (although it depends on the host bacteria) (Principi et al., 2019). Also, phages are

thought to be significantly safer and better tolerated than antibiotics, since they replicate only in the target bacteria but are innocuous to mammalian cells (Kakasis & Panitsa, 2019). Furthermore, their administration is easier, as phages do not need repeated administrations over several days, as is commonly required for antibiotics, because they can remain in the human body for relatively long periods of time. Also because phages have the ability to self-replicate, increasing their number where they are needed. Unlike antibiotics, their effect is limited to the local of infection that can be reached, even when the bacteria are located in an organ or system of the body that antimicrobials are unlikely to penetrate (Loc-carrillo & Abedon, 2011; Principi et al., 2019). Another advantage of using phages is that they can be less expensive than antibiotics as their production is relatively simple and affordable.

Finally, phages can even be used to disperse bacterial biofilms, which are extremely difficult to eradicate with standard antibiotic therapy, even if the bacteria are sensitive to the drug being administered. *In vitro* studies demonstrated that a combination of phages with other antimicrobial agents such as antibiotics and antiseptics, in the vast majority of cases increases biofilm eradication compared to antibiotic/antiseptic alone (Pires et al., 2017; Principi et al., 2019). Additionally, the combined treatments can usually significantly restrict the formation of resistant variants compared to each treatment alone (Pires et al., 2017). It was also described that, in most cases, the use of phages before antibiotics results in the maximum eradication of *P. aeruginosa* biofilms *in vitro*. Furthermore, several studies also reported the use of phage cocktails combining multiple phages, preferably directed to different receptors and with complementary host ranges in a single preparation, as a strategy in the treatment of bacterial biofilms (Pires et al., 2017; Principi et al., 2019). This approach can be applied to prevent bacterial colonization and biofilm formation, which can inhibit the development of bacterial infections. Besides that, phages can be genetically manipulated to enhance their antibiofilm activity as described by Lu & Collins, (2007).

On the other hand, one of the main concerns that may decrease the efficacy of phage therapy, is the possible emergence of bacteriophage insensitive mutants (BIMs) during treatment. Mechanisms of phage resistance in bacteria include: blocking phage adsorption to bacterial receptors; preventing the entry of phage DNA by superinfection exclusion systems; cleavage of genomic phage DNA by restriction modification systems (RM), Clustered Regularly Interspaced Short Palindromic Repeats (CRISPR) and associated Cas; use of abortive infection systems that block phage replication, transcription or translation; or anti-phage signalling systems based on cyclic oligonucleotide (Pang et al., 2019; Pires et al., 2020).

However, bacterial resistance to phages can be circumvented using different approaches (Pires et al., 2020). The most common is the use of phage cocktails targeting multiple receptors (Pirnay et al., 2011). Another strategy commonly in therapy is to replace the phage for which the bacterium has developed resistance with a phage that is active against the resistant variant. Although this is not easy for antibiotics, when it comes to phages it can be quite simple, given its abundance and diversity in nature, as a result of its constant coevolution with bacteria (Rohde et al., 2018). Finally, the combination of phages with antibiotics or other antimicrobial agents can also be used to arrest the development of bacterial resistance and to improve the therapeutic outcome (Pires et al., 2020; Tagliaferri et al., 2019; Torres-Barceló, 2018).

The above mentioned limitations of phages require the design of strategies to improve their properties and therapeutic characteristics. Synthetic biology has allowed great advances in this area and phage-engineering has been successfully used to modulate the phages' host range (Ando et al., 2015), reduce phage toxicity and immunogenicity (Hagens et al., 2004; Matsuda et al., 2005), increase phage survival after administration, improve phage activity against biofilms (Lu & Collins, 2007; Waters et al., 2017), and increase bacterial death when combined with antibiotics (Lu & Collins, 2009).

1.3.3. Diagnosis of pathogens based on phages

The development of rapid methods for the detection and identification of pathogens is essential to improve the prevention and treatment of bacterial diseases in various fields, from food production to health care. Although culture-based detection remains the gold standard for the detection and identification of bacterial pathogens, it can be laborious and time-consuming, typically requiring more than 48 hours to allow selective bacterial growth and ensure a reliable detection. Immunologic and DNA-based techniques also require a lot of time, are expensive, have high detection limits, and frequently show cross-reactivity. Therefore, robust and sensitive alternatives for diagnostic are needed and a promising tool may be the implementation of phage-based diagnostics (Meile et al., 2020).

The ability of phages to specifically infect bacteria can be exploited towards the development of effective detection methods, including capturing cells by immobilized phages and tagging target organisms by fluorescence-labelled phage particles (Santos et al., 2020). Whole-phage particles are used as bioprobes in biosensors due to their high binding affinity. They have the advantage of detecting living, metabolically active cells and can also be conjugated with magnetic nanoparticles, radioactive tracers, fluorophores, or a mix of these to label and enrich bacteria for detection (Meile et al., 2020).

The alternative to whole phage bioprobes is to use phage proteins that confer binding to the host. Phages recognize their bacterial hosts using specialized RBPs, usually identified as Tail Fiber Proteins (TFPs), which initiate the binding of the phage to specific receptors on the bacterial cell wall. TFPs are remarkable biorecognition components, due to their ability to detect specific pathogens. Furthermore, they are responsible for the high selectivity conferred to the phages against bacteria (Meile et al., 2020; Santos et al., 2020). However, TFPs do not discriminate between living or dead cells as long as the bacterial cell is complete. (Santos et al., 2020). Other phage-encoded molecules, such as cell wall binding domains of phage endolysins are also suitable for detection purposes when coupled with the magnetic separation for capturing bacteria. Although these phage-based proteins have been used for pathogen detection, the use of reporter phages have the advantage of self-replicate in the host, increasing the signal along the time and consequently, decreasing the detection limit. Bioluminescence-based reporter phages are genetically modified viruses that carry a heterologous luciferase gene whose activity can be detected with high sensitivity to indicate the presence of viable target cells. Luciferases are the most sensitive reporter genes and have been used to build a series of reporter phages that allow the detection of *Pseudomonas*, *Listeria*, *Mycobacterium*, *Bacillus*, *Yersinia*, *Escherichia*, *Salmonella* and *Erwinia* species (Meile et al., 2020).

In conclusion, the use of phages for the detection of pathogenic bacteria offers interesting advantages compared to traditional analytical methods (Schmelcher & Loessner, 2008). However, it is important to note that, while some phages have wide host ranges, others are very limited to a narrow range of bacterial strains (Koskella & Meaden, 2013; Motlagh et al., 2016). Particularly, *P. aeruginosa* phages typically display limited host ranges, which constitutes a disadvantage for detection purposes as it does not allow the identification of numerous strains. This bottleneck can be overcome by phage-engineering, allowing the increase the host spectrum. This requires the identification of phage TFPs with complementary spectra and their subsequent cloning into a phage genome to broaden the host range and consequently, improve detection.

1.3.4. Phage-engineering techniques

The development of new phage-engineering techniques has increased in the past decade (Pang et al., 2019). These tools allow the design of chimeric/synthetic phages “a la carte”, in order to circumvent the limitations raised by the natural phages. Therefore, chimeric phages may soon be at the frontline of the fight against lethal pathogens that are drug-resistant. (Nair & Khairnar, 2019).

One of the oldest methods for engineering phage genomes is homologous recombination in their bacterial hosts, which can occur between two homologous DNA sequences. Homologous recombination is a naturally occurring phenomenon. It allows cells to recombine heterologous DNA introduced into cells with their own genomic DNA, when both sequences share regions of homology. This principle can be used to manipulate phage genomes inside the host and has been applied to incorporate foreign genes into phage genomes. However, when the goal is to obtain multiple mutations, each mutation is often done sequentially and independently, which is a time-consuming process. In addition, usually only a small percentage of the progeny phages will be recombinant and so, the screening process is very difficult unless a reporter gene is used (Pires et al., 2016).

Another strategy often used for phage genome engineering is the bacteriophage recombineering of electroporated DNA (BRED). This technique can be used to delete, insert and replace genes, as well as create point mutations in phage genomes. BRED consists of co-electroporating the recombination substrates (phage DNA and double-stranded DNA (dsDNA)) into electrocompetent host cells that carry a plasmid encoding proteins that promote high levels of homologous recombination. This technique requires highly competent bacterial hosts and usually yields low rates of recombinant phages (but higher than homologous recombination) (Pires et al., 2016).

CRISPR-Cas systems can also be used to engineer phage genomes. CRISPR-Cas forms an "adaptive" immune system in bacteria and archaea, protecting microbial cells from invasion of foreign DNA, such as DNA delivered by invading phage genomes (Pang et al., 2019). The use of CRISPR-Cas systems can be combined with homologous recombination technique to counter-select the recombinant phages from a mixed population with wild-type and recombinant phages, thus overcoming the problem of having to select a very small percentage of recombinant phages from a large pool of wild-type phages (Pires et al., 2016).

Since the propagation of phage genomes in a bacterial host can be toxic to the host, thus limiting the efficiency of phage genome engineering with methods such as homologous recombination or BRED, this problem can be overcome by using yeast instead of bacteria as an intermediate host for genetic manipulation. Homologous recombination is particularly efficient in *Saccharomyces cerevisiae*, and phage genomes do not cause yeast toxicity and can be maintained in a stable manner. In this technique the phage is manipulated and captured into a yeast artificial chromosome. After, the yeast-phage genome is extracted and transformed into the bacterial host to generate functional phages. Although this

technique has been used to manipulate phages targeting several bacterial species, its efficiency is also restricted by the transformation efficiencies of the host (Pires et al., 2016).

Although highly efficient transformation protocols have been designed for some bacteria, such as *E. coli* and *P. aeruginosa*, many other bacterial species are extremely difficult to transform. This represents a bottleneck in the yield and efficiency of several phage-engineering systems and cell-free transcription-translation systems may offer a potential solution to this problem (Pires et al., 2016).

Until now, the only technique that has been applied to manipulate the genomes of *P. aeruginosa* phages was the yeast-based phage-engineering platform. Using this approach, Pires et al. (2021) generated chimeric phages with reduced genomes by knocking out up to 48% of the genes with unknown functions from the genome of the *P. aeruginosa* phage vB_PaeP_PE3. On the other hand, they also studied whether the genomic deletions made on phages influence their performance. Overall, the authors assembled 3 chimeric phages lacking different sets of genes encoding hypothetical proteins and, although they found that these sets of genes were unnecessary for phage viability and replication, some of the genes could play an important role in the early stage of phage infection. Nonetheless, in vitro and *in vivo* infection assays showed no differences between the wildtype and the chimeric phages. The elimination of unnecessary genes is an interesting approach as it creates some space in the phage genomes, allowing the introduction of other genes of interest that can potentiate their antibacterial activity (Pires et al., 2021).

The phage designated as PE3Δgp1–gp12 throughout this work consists of a phage previously assembled by Pires et al., (2021) and the phage PE3Δgp1–gp12:Nluc is a modification of the PE3Δgp1–gp12 by the insertion of the Nanoluc reporter gene after the endolysin gene. Nanoluc (Nluc) is a modified luciferase derived from a deep-sea luminous shrimp. This enzyme is small, stable, and produces bright, sustained luminescence (Dixon et al., 2016). In brief, genetically modified phages can have significant benefits for the diagnosis as well as for the treatment of bacterial infections.

1.4. Project aims

P. aeruginosa is one of the most common causes of infections in hospitalized patients. This Gram-negative bacterial pathogen presents a serious therapeutic challenge due to its high resistance to a wide range of antibiotics, which results in prolonged hospital stays, increased medical costs and high mortality rates. In an era where antibiotic resistance is one of the highest threats to human health, phages have great potential against bacterial diseases. Although, phages generally have a limited host range,

being able to infect only a limited number of strains within a genus or even species, a problem that is usually solved by developing cocktails from natural phages, which is a lengthy and laborious process. However, using phage-engineering tools, it is possible to overcome this problem and assemble chimeric phages with expanded host ranges and, therefore, capable of reaching a wider range of strains. These phages can also encode reporter genes, resulting in a fast and accurate tool for the detection of bacteria in clinical settings, thus replacing conventional culture methods that are time-consuming.

Along these lines, additionally to the increasing knowledge in the area, the aim of this project relies on genome engineering of *P. aeruginosa* phages to improve its functionalities, such as the increase of the host spectrum to target a wider range of strains and to incorporate reporter genes that allow their simple use as a sensitive and reliable detection tool. The resultant chimeric phages are expected to enhance therapy and diagnosis of *P. aeruginosa* infections.

Chapter 2

MATERIALS AND METHODS

2. MATERIALS AND METHODS

2.1. Strains, plasmids and culture conditions

All the strains, bacteriophages and plasmids used in this work are listed in **Supplementary material - Table S1**. The clinical isolates were provided by the Hospital of Braga (Portugal).

All bacterial strains were grown in Lysogeny Broth (LB) (Nzytech) at 37 °C under agitation (120 rpm) or in LB agar (LBA) plates, obtained by adding 12 $g \cdot L^{-1}$ of agar (Lioflchem). All media were prepared according to the manufacturer's instructions and autoclaved before use. Due to the facility to be manipulated and the high pool of tools available for this organism, *Escherichia coli* was used for cloning and heterologous expression. The *E. coli* strain growth media were supplemented with antibiotics for selection when necessary: kanamycin (Nzytech) at 50 µg/mL and gentamicin (Nzytech) at 20 µg/mL, and the bacterial growth was determined by measuring the optical density at 600nm (OD_{600nm}) in 96-well plates (Orange Scientifc) using a Multiskan™ FC Microplate Photometer (ThermoFisher Scientifc).

Chemically competent (QC) cells were prepared for the following strains: *E. coli* Arctic Express (AE)(DE3), C43 (DE3) and BL21 (DE3). For this, the *E. coli* strain was grown overnight at 37 °C, 120 rpm in 10 mL of LB. This culture was diluted 1:100 in fresh LB and incubated at 37 °C, 120 rpm for 1 h 30 min. Following centrifugation (3300 ×g, 4 °C, 10 min), the cells were collected, resuspended in half of the initial volume of ice-cold 0.1 M $CaCl_2$, and stored on ice for 30 min. After a second centrifugation (3300 ×g, 4 °C, 10 min), the pellet was resuspended in 1/10 of the initial volume of ice-cold 0.1 M $CaCl_2$. Finally, another centrifugation (3300 ×g, 4 °C, 10 min) was carried and the pellet resuspended in 1 mL of ice-cold 0.1 M $CaCl_2$ and aliquots of 50 µL were made and stored at -80 °C until use.

Transformant AE cells were inoculated in LB broth supplemented with Kanamycin and gentamicin, at 16 °C, 160 rpm while C43 and BL21 cells were inoculated in LB broth supplemented only with kanamycin. C43 cells were cultured at 21 °C and 160 rpm and BL21 cells were cultured on the same conditions as AE.

The constructions of the recombinant plasmids were predicted using the SnapGene™ 1.1.3 version Software. All bacteria (with or without the correct constructs) were stored at -20 °C in LB broth supplemented with 20 % glycerol (v/v).

The *Saccharomyces cerevisiae* BY4741 (MATa his3Δ1 leu2Δ0 met15Δ0 ura3Δ0) and the yeast centromere vector pRS415 (ATCC 87520) with LEU2 marker were obtained from laboratory stocks. *S. cerevisiae* BY4741 was cultured in YPD (1 % (w/v) Bacto Yeast Extract, 2 % (w/v) Bacto Peptone and

2 % dextrose (w/v)) or YPD agar at 30 °C. All clones (yeast transformants) with the proper gene size were stored at -20 °C in SD-Leu [0.67 % Yeast Nitogen Base (YNB), 0.069 % CSM-Leu, 2 % dextrose] supplemented with 20 % glycerol (v/v).

2.2. Sensitivity tests for detection of *P. aeruginosa*

The sensitivity of a previously assembled reporter phage (designated as PE3Δgp1–gp12:Nluc) was assessed here to determine the detection limit of the phage. This phage consists in the PE3Δgp1–gp12 phage with the Nanoluc reporter gene, which was inserted after the endolysin gene.

Cultures of *P. aeruginosa* PAO1 grown overnight in LB medium were nine-fold serially diluted and infected with 10^5 PFU/mL of the reporter phage PE3Δgp1–gp12:Nluc. Bacterial counts from each dilution were determined by plating on LB agar prior to infection. Infected cultures (50 µL) were incubated at 37 °C with agitation (120 rpm) and bioluminescence was quantified at time 0 and every hour, during a period of 7 hours, in eppendorf tubes using a Ultrasensitive Single Tube Luminometer (Promega) after the addition of Nano-Glo® Luciferase (Promega) reagent according to the manufacturer's instructions. **Figure 3** shows the procedure of the sensitivity tests in a schematic way.

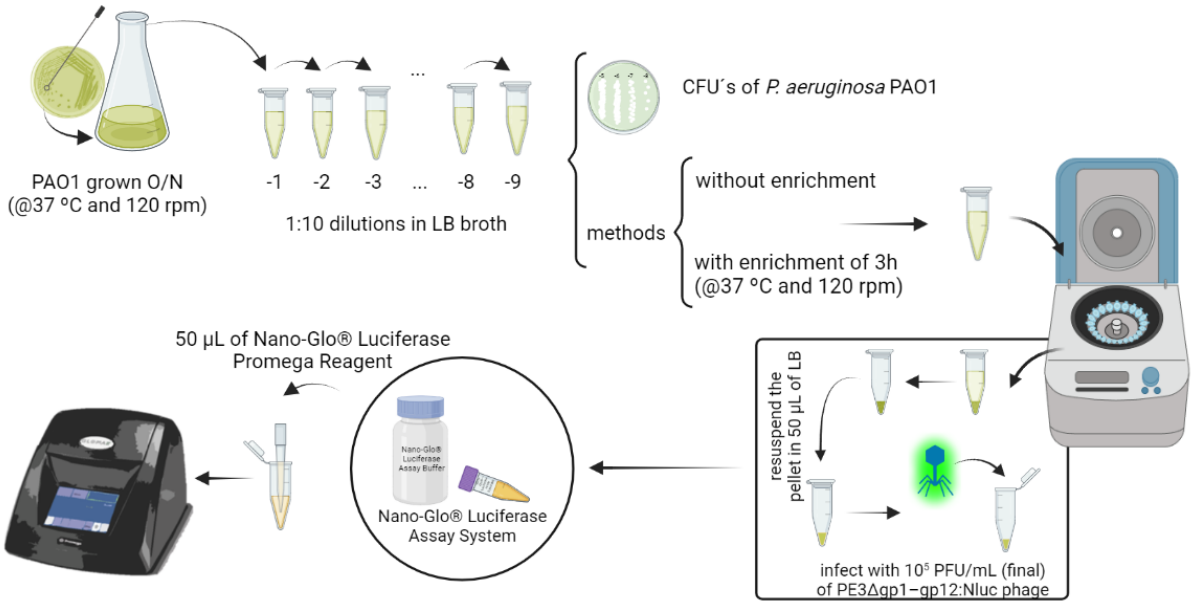

Figure 3 - Procedure followed for the sensitivity tests, for the detection of *P. aeruginosa*.

In non-enrichment experiments, the bacterial cultures were infected with phage immediately after dilutions, and the luminescence signal (RLUs) was tracked over time (maximum of 7 h). In enrichment

assays, the dilutions of the bacterial culture were incubated at 37°C for three hours before being infected with phage for 4 hours.

The methodology was repeated for some clinical strains of *P. aeruginosa* (5, 6, 16, 21, 23, 27, A65, 065, 092 and PA14 – listed in **Supplementary material - Table S1**) and for clinical strains of *E. coli* (A51), *Klebsiella pneumoniae* (A36, A57), *Staphylococcus aureus* (A1, A9, A39), *Enterococcus faecalis* (A74), and *Enterococcus faecium* (A78), also listed in **Supplementary material - Table S1**.

2.3. Evaluation of lytic spectra and efficiency of plating

To evaluate the lytic spectrum of phages, one drop (5 µL) of each phage sample was added to the bacterial lawns and incubated overnight at 37 °C. The bacterial lawns were prepared by mixing 100 µL of bacterial suspensions with 3-5 mL of LB soft agar (LB with 0.6 % (w/v) of agar) into a LBA plate. After incubation, the host range was determined by visualizing the presence of lysis zones, suggesting the phage's ability to infect the host (Pires et al., 2021; Ribeiro et al., 2019). If a lysis zone was observed in the spot test, then the efficiency of plating (EOP) of the respective phage was assessed by plating serial dilutions of the phage stock on the bacterial lawns that previously showed a lysis zone. After overnight incubation at 37 °C, the resulting Plaque forming units (PFU's) were counted. The EOP (average PFU on target bacteria / average PFU on host bacteria) was then determined (**Table 17**).

When the ratio was 0.5 or higher, meaning that the infection on the target bacteria produced at least 50 % of the PFU reported for the primary host, the average EOP value for a certain phage-bacterium combination was classed as "High production". EOP values between 0.001 and 0.1 were categorized as "Low production" efficiency, while values greater than 0.1 but less than 0.5 were classified as "Medium production" efficiency. An EOP of 0.001 or less was considered inefficient (Mirzaei & Nilsson, 2015). Based on the analysis of the lytic spectra, 2 phages with complementary host ranges were selected for the next tasks.

2.4. Cloning and functional analysis of potential TFPs

Tail fiber proteins identified during the genome analysis were selected based on the existence of homologs deposited in the NCBI database of non-redundant proteins identified through BLASTp and also on homologs to the predicted structure using HHpred. In addition, the predicted functional domains, the

molecular weight, and the isoelectric point of the proteins were identified and calculated using bioinformatics analysis tools (Costa et al., 2020; Santos et al., 2020).

2.4.1. Gene amplification

Seven different genes were selected (nucleotide and amino acidic sequence of the selected genes are available in **Supplementary material – Table S2)**. Primers containing specific restriction cloning sites were designed to amplify the genes encoding the recombinant proteins and to insert them into the pGFP plasmid. This plasmid consists in a construction of the commercial plasmid pET28a(+) (Novagen's), that carries the T7 promoter, a 6× His-tag N-terminal, a kanamycin resistant marker and a lac promoter, with the synthetic construct aceGFP (*Aequora coerulescens* Green Fluorescent Protein gene. GenBank: AY233272.1) inserted in the multiple cloning site (MCS) between the *Nde*I and *BamH*I restriction enzymes sites (**Figure 4**) (Costa et al., 2020). aceGFP is a commonly used tool in molecular biology, medicine and cell biology, as it can be used as biological marker. Furthermore, fusion of aceGFP to a protein does not usually change the function or location of the protein and combines a number of advantageous traits, including high stability, minimal toxicity, and the ability to induce fluorescence when excited at a proper wavelength, eliminating the need for a substrate as is necessary for luciferases (Schmelcher & Loessner, 2014).

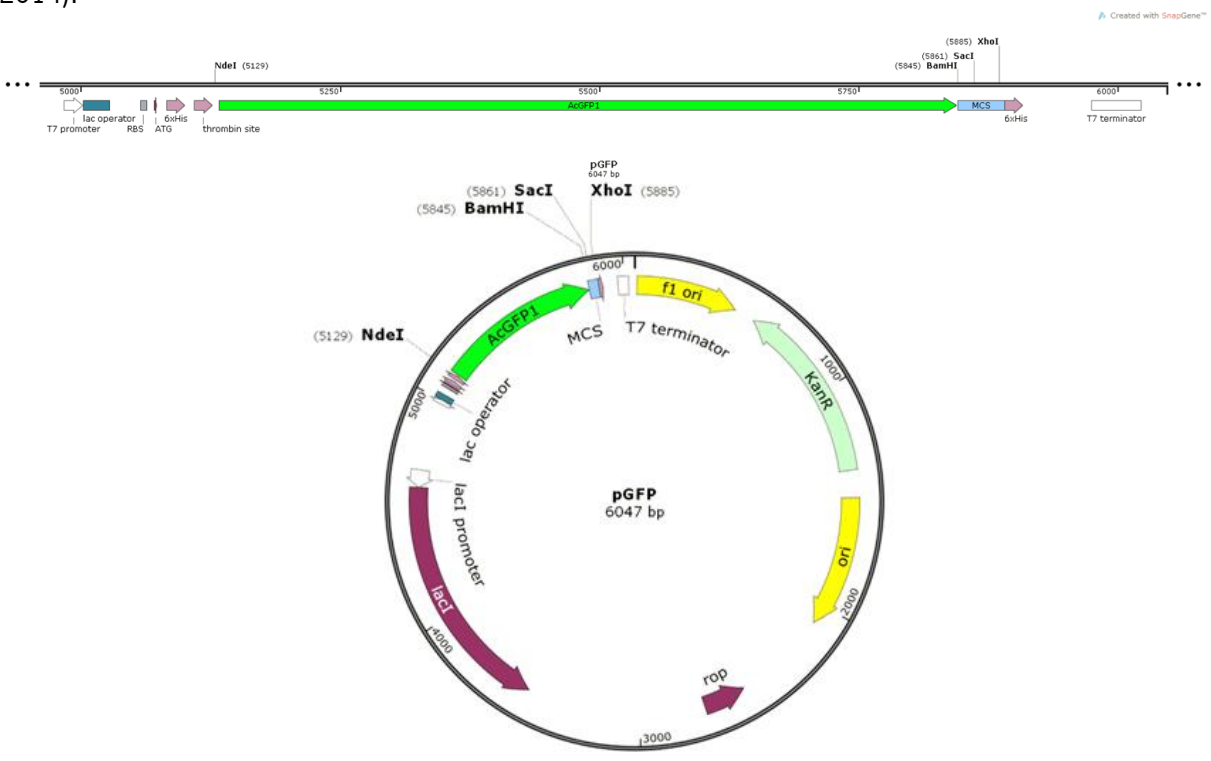

Figure 4 – General features of pGFP vector, used for cloning and expression of the TFP genes. pGFP vector contains the same features as pET28a+ (Novagen) with the addition of the aceGFP gene.

The TFP genes were inserted between the *Sac*I and *Xho*I restriction sites since these enzymes do not cut the TFP coding sequences as predicted with SnapGene™ 1.1.3. The use of two different restriction enzymes was used to prevent the plasmid from recirculating cleavage and to ensure the insertion of the TFP gene in the correct direction.

The primers (**Table 1**) were designed to include at the 5' end the enzyme restriction sites (underlined) and some nucleotides that were added to optimize enzyme activity (CG repeats). SnapGene™ 1.1.3 was used to determine some parameters as the melting temperature (Tm) and the GC content.

Table 1 - Primers used to amplify the TFPs encoding genes from phiIBB-PAA2 and vB_PaeP_PE3 phages, the respective restriction enzyme site used and their parameters. Tm represents the melting temperature. Enzyme restriction sites are underlined

Gene	Sequence (5'→3')	Enzyme	Tm (°C)	GC content (%)
A2gp53	Fw: GCCGCCGAGCTCATGAGTCAAAAGTACAGCCCTTCG	*Sac*I	56	46
	Rv: CCGCCGCTCGAGTCATGGAGTCACCACCAGGG	*Xho*I	56	60
A2gp55	Fw: GCCGCCGAGCTCATGGGTCTTGAGGTCGCAAC	*Sac*I	54	55
	Rv: CCGCCGCTCGAGTCAGTTCTTAATGATGAAGAACACAG	*Xho*I	53	35
PE3gp39	Fw: GCCGCCGAGCTCATGCTACTACTCGACGCAGTG	*Sac*I	69	64
	Rv: CCGCCGCTCGAGTCAGGTCCTCAAGCTGCGC	*Xho*I	72	71
PE3gp44	Fw: GCCGCCGAGCTCGTGGCTCGGTTCAAGAATCC	*Sac*I	54	55
	Rv: CCGCCGCTCGAGTTATTCGTCCTCCATGGCCC	*Xho*I	54	55
PE3gp45	Fw: GCCGCCGAGCTCATGCGCGGCATTATCGCGG	*Sac*I	55	63
	Rv: CCGCCGCTCGAGTTAAACATTTTTCAGCTCCGCCTG	*Xho*I	54	42
PE3gp46	Fw: GCCGCCGAGCTCATGTTTAAGACCGAAGTAAAGGGACG	*Sac*I	56	42
	Rv: CCGCCGCTCGAGTTATGCCCTCGCCACCGTAAAC	*Xho*I	57	55
PE3gp47	Fw: GCCGCCGAGCTCATGGCACTGATCTACGACTTCAAC	*Sac*I	56	46
	Rv: CCGCCGCTCGAGTTACATGTGCCCTCTGAATTGGAC	*Xho*I	56	46

DNA fragments were amplified with Phusion™ Plus DNA Polymerase (ThermoFisher Scientific) that has proof reading activity in order to reduce the insertion of incorrect nucleotides, using phage phiIBB-PAA2 (short name A2) as template DNA for genes 53 and 55, and phage vB_PaeP_PE3 (short name PE3) as template DNA for genes 39, 44, 45, 46 and 47. The PCR mix components were adjusted

according to the manufacturer's instructions (**Table 2**) and the PCR amplification was performed on a T100™ Thermal Cycler (BioRad).

Table 2 - Components and quantities used for PCR with Phusion™ Plus DNA Polymerase

Components	Concentration
Phusion Plus DNA Polymerase	0.02 U/µL
5× Phusion Plus Buffer	1×
dNTP mix (10mM)	200 µM
Primers	0.5 µM
Template DNA	0.9 ng/µL
Water, nuclease free	to 50 µL

The thermocycling conditions for the PCR are shown in **Table 3**.

Table 3 - Thermocycling conditions for a routine PCR with Phusion™ Plus DNA Polymerase

Step	Temperature	Time
Initial Denaturation	98 °C	5 min
25-35 Cycles	98 °C	10 sec
	55 °C or 60 °C	10 sec
	72 °C	15-30 sec/Kb
Final Extension	72 °C	5 min
Hold	12 °C	

Confirmation of PCR products was performed through agarose gel electrophoresis. The gels contained 1 % (w/v) agarose (Nzytech) dissolved in 1× TAE buffer (1 mM ethylenediamine tetraacetic acid (EDTA); 40 mM Tris base; 20 mM acetic acid) and were stained with GreenSafe Premium (Nzytech). The 1 Kb GRS Ladder DNA (Grisp) was used as a marker. Electrophoresis was performed in 1× TAE buffer at 100 V for 40 min in a PerfectBlue gel system (VWR) and the gels were visualized using a ChemiDoc™ XRS (BioRad) equipment with Image Lab™ 5.1 software (BioRad). Then, the PCR products were purified using the DNA Clean and Concentrator kit (Zymo Research) and the DNA concentration of the amplified

fragments was determined using the NanoDrop™ One Microvolume UV-Vis Spectrophotometer (ThermoFisher Scientific).

2.4.2. Cloning

Plasmid and PCR products were digested with two FastDigest Restriction Enzymes *Sac*I and *Xho*I (ThermoFisher Scientific), creating sticky ends complementary between the vector and the insert. The reaction components were adjusted according to the manufacturer's instructions and are shown in **Table 4**. Digestions were performed at 37 °C for 2 h and inactivated in a HeatBlock (VWR) at 82 °C for 6 min.

Table 4 - Reaction components and volumes or concentrations used to digest the target genes

Components	Volume
10× FD Buffer	2 µL
DNA insert or DNA plasmid	200 ng or 1000 ng
SacI FD	1 µL
XhoI FD	1 µL
Water, nuclease free	to 20 µL

Digested products were cleaned with the DNA Clean and Concentrator Kit (Zymo Research) according to the manufacturer's instructions and DNA concentration determined using the NanoDrop™ One Microvolume UV-Vis Spectrophotometer (ThermoFisher Scientific).

After digestion, the genes were inserted into pGFP (to fuse them with the upstream aceGFP) using the T4 DNA Ligase (ThermoFisher Scientific), according to the manufacturer's instructions (**Table 5**), to ligate DNA fragments with cohesive ends, obtaining different constructs. The ligation mixture was incubated at room temperature for 2 h and the reaction stopped by a subsequent incubation at 72 °C for 6 min. To reduce background (non-digested pGFP), a subsequent digestion step was performed with 0.5 µL of *Sal*I (ThermoFisher Scientific) and 1 µL of the respective buffer (ThermoFisher Scientific), followed by incubation at 37 °C for 45 min. The *Sal*I enzyme was further inactivated at 80 °C for 5 min.

Table 5 - Reaction components, volumes or final concentrations for the ligation of the target genes

Components	Volume
Linear vector DNA (plasmid)	20-100 ng
Insert DNA (gene)	1:1 to 5:1 molar ratio over vector
10× T4 DNA Ligase Buffer	2 µL
T4 DNA Ligase	1 Weiss U
Water, nuclease free	to 20 µL

The primer design, gene amplifications, digestions and ligations were all simulated *in silico* using the SnapGene™ 1.1.3 version Software.

The recombinant plasmids pGFP_A2gp53, pGFP_A2gp55, pGFP_PE3gp39, pGFP_PE3gp44, pGFP_PE3gp45, pGFP_PE3gp46 and pGFP_PE3gp47 consist in the insertion of the putative TFP encoding genes *gp53* and *gp55*, from phiIBB-PAA2 phage, and *gp*39, *gp*44, gp*45*, gp*46* and *gp*47, from vB_PaeP_PE3 phage, in the pGFP plasmid. These plasmids were transformed into competent *E. coli* AE (DE3) cells by heat shock.

Briefly, for the transformation of the plasmids, 5 µL of ligation was mixed gently with an aliquot of chemically competent cells. After 20-30 min on ice, a heat shock was performed: 50 sec at 42 °C and 2 min on ice. Then, 300 µL of SOC (Super Optimal broth with Catabolite repression) was added to the tube and the cells were allowed to recover for 1 h 30 min at 37 °C. Then, the suspension was spread on LB agar petri dishes containing kanamycin (50 µg/mL) and gentamicin (20 µg/mL) for QC AE (DE3) cells. The plates were incubated overnight at 37 °C and checked for the presence of transformed colonies.

The resulting transformed colonies were subjected to colony PCR to assess correct assembly (cells that incorporated the recombinant vector) before the confirmation by Sanger sequencing. Colonies were randomly selected and resuspended in 25 µL of LB broth with the corresponding antibiotic(s) to be used as a template in the PCR reaction. The PCR reaction was performed using the Xpert Fast Hotstart Mastermix (2×) (Grisp) where the T7 primers were added and the reaction was adjusted according to the manufacturer's recommendations (**Table 6**).

Table 6 - PCR mix components and their final concentrations for colony PCR

Components	Concentration
Xpert Fast Hotstart Mastermix (2×) with dye (Grisp)	1×
T7 Forward primer	0.4 µM
T7 Reverse primer	0.4 µM
Template DNA	1-250 ng
Water, nuclease free	to 6 µL

T7 Mastermix (2×) with dye (Grisp) consists on the Xpert Fast Hotstart, supplied as a convenient 2× mastermix and which includes an electrophoresis inert tracking dye, containing all components necessary for fast PCR and the T7 forward and reverse primers (specific for the pGFP plasmid, showed on **Table 7**).

Table 7 - Primers used for colony PCR and their parameters. Tm represents the melting temperature

Primer	Sequence (5'→3')	Size (bp)	Tm (°C)	GC content (%)
T7 forward	TAATACGACTCACTATAGGG	20	47.7	40
T7 reverse	GCTAGTTATTGCTCAGCGG	19	51.1	53

PCR amplification was performed in a DNA thermocycler (T100™ Thermal Cycler (BioRad)) and the PCR protocol is described in **Table 8**.

Table 8 - Thermocycling conditions for a colony PCR

Step	Temperature	Time
Initial Denaturation	95 °C	5 min
35 Cycles	95 °C	15 sec
	49 °C	15 sec
	72 °C	30 sec
Final Extension	72 °C	5 min
Hold	12 °C	

The PCR product was run on a 1 % (w/v) agarose gel to analyze the size of the product and assess correct gene insertion. Clones that contained the correct size of the gene were spread on LB agar plates with appropriate antibiotic and incubated overnight at 37 °C. Recombinant plasmids were extracted using the NucleoSpin® Plasmid kit (Macherey-Nagel™), the concentration was quantified in a NanoDrop™ One Microvolume UV-Vis Spectrophotometer (ThermoFisher Scientific) and then sent for sequencing at Eurofins Scientific, to confirm the correct gene insertion and the absence of mutations.

2.4.3. Protein expression

For protein expression, the correct plasmid needs to be cloned into a suitable expression strain. The competent strain *E. coli* AE (DE3) was used to express the protein. Small-scale expression experiments of 50 mL were performed to assess the solubility of the recombinant proteins and perform the protein functional analysis. Briefly, AE (DE3) cells were inoculated into LB broth supplemented with the respective antibiotics and incubated overnight at 37 °C, 120 rpm. The next day, the culture was diluted 1:100 in LB broth and incubated at 37 °C at 120 rpm until the OD_{600nm} reached 0.5. Then, the expression of the recombinant protein was induced with 50 µL of isopropyl β-D-1-thiogalactopyranoside (1 mM IPTG, ThermoFisher Scientific) and the proteins were expressed for 24 h at 16 °C, 160 rpm in a Cooled Incubator MIR-254 (Parasonic). To recover the expressed proteins, the culture was centrifuged at 9000 ×g for 10 min at 4 °C and the bacterial cell pellet was resuspended in 10 mL of 1× Lysis Buffer (0.5 M NaCl, 20 mM of NaH_2PO_4/NaOH, pH 7.4). Cells were disrupted with a combination of 3 freeze-thaw cycles (-80 °C/30 °C) and 5 min sonication (30 second pulses ON, 30 second pulses OFF, 40 % amplitude intensity, on Cole-Parmer Ultrasonic Processor) on ice to prevent protein denaturation. The resulting suspension was centrifuged at 9000 ×g for 15 min and the supernatant containing the soluble protein was filtered with a 0.45 µm membrane filter to remove large bacterial debris.

In cases where the protein was not well expressed, the heterologous expression was repeated in different cells, such as C43 (DE3) and BL21 (DE3).

2.4.4. Protein purification

Expressed proteins were purified through a nickel-nitrilotriacetic acid (Ni^{2+}-NTA) resin affinity chromatography column (ThermoFisher Scientific) since the fusion proteins were expressed carrying a N-terminal His-Tag. After washing (lysis buffer supplemented with 30 mM imidazole) to remove non-specific

binding of proteins to the purification matrix, proteins were eluted with 300 mM imidazole. Purified proteins were analysed by sodium dodecyl sulfate – polyacrylamide gel electrophoresis (SDS-PAGE) (12.5 % (w/v) acrylamide). Following the assembly of the SDS system, the Resolving Gel (12.5 %) and the Stacking Gel were made in accordance with **Table 9**.

Table 9 - SDS-PAGE components and quantities

Reagents	Resolving gel	Stacking gel
Water, nuclease free	2.19 mL	1.57 mL
1.5 M Tris-HCl pH 8.8	1.25 mL	-
1.5 M Tris-HCl pH 6.8	-	0.63 mL
40 % Acrylamide/Bis-Acrylamide	1.56 mL	0.31 mL
SDS	25 µL	15 µL
10 % APS	50 µL	25 µL
TEMED	5 µL	2.5 µL
Total	5 mL	2.5 mL

Samples were prepared for analysis by adding 16 µL of the sample to 4 µL of 5× SDS-PAGE Sample Loading Buffer (Nzytech) and heated the mixture at 95 °C for 5 min. Then, the prepared samples were loaded onto the gel. The NZYColour Protein Marker II (Nzytech) and the PageRuler™ Broad Range Unstained Protein Ladder (ThermoFisher Scientific) were used. The electrophoresis was carried out in 1× TGS (Tris-Glycine-SDS) buffer and the power supply was automated for 30 min at 80 V and 90 min at 120 V. The gels were stained using BlueSafe protein stain (Nzytech) and the revealed bands were analyzed.

In the case of expression of insoluble proteins (proteins which accumulated in the pellet of centrifugated samples after cell lysis), the pellet was resuspended in 5 mL 1× Lysis Buffer, then centrifuged at maximum speed for 5 min at 4 °C and the supernatant discarded. Three washes were performed, two with 3 mL of 0.5 % TritonX-100 and the last one with 3 mL of 1× Lysis Buffer. To solubilize the protein, the pellet is resuspended in 3 mL of PBS pH 7.4 with 8 M urea. Then, the protein was incubated for 12 h with gentle shaking (60 rpm) at room temperature, the inclusion bodies were recovered by centrifugation at maximum speed for 10 min at 4 °C and the supernatant was filtered and stored at 4 °C. The last step of the pellet solubilization process was dialysis, performed into a Membra-Cel® MD10

dialysis membrane with molecular cut-off of 14 KDa (Viskase) previously hydrated in distilled water, using decreasing concentrations of urea. The next day, the dialyzed protein was recovered and tested again.

2.4.5. Fluorescence microscopy

The binding capacity of the different GFP-fused proteins (pGFP_A2gp53, pGFP_A2gp55, pGFP_PE3gp39, pGFP_PE3gp44, pGFP_PE3gp45, pGFP_PE3gp46 and pGFP_PE3gp47) was inferred by fluorescence microscopy observations. Briefly, *P. aeruginosa* PAO1 cells were grown overnight in 1 mL of LB at 37 °C and then 20 µL of the culture was incubated with the fused proteins for 15 min at room temperature. Cells were washed with 100 µL of 1× Lysis Buffer and then centrifuged (9000 ×g, 5 min) to remove unbound protein. The washed pellet was resuspended in 100 µL of 1× Lysis Buffer and a 10 µL drop observed under an epifluorescence microscope equipped with a U-RFL-T light source (Olympus BX51, Magnification 1000×) in bright field and under the FITC filter (Excitation BP 470–490 nm; Emission: LP 516 nm) (Costa et al., 2020).

2.5. Genome engineering of *P. aeruginosa* phage vB_PaeP_PE3

The genome engineering of PE3 phage was done using the yeast-based phage-engineering platform already optimized for this phage (Pires et al., 2021). The goal here was to clone an additional TFP (*gp*55) from phage phiIBB-PAA2 (short name A2) into PE3 phage, in order to expand the host range of the phage. Tranformation 1 (T1) consists on the insertion of the TFP gene *gp*55 in the phage PE3Δgp1–gp12 between the TFP gene *gp48* and the TFP gene *gp49* and Transformation 2 (T2) consists in the insertion of the same gene in PE3Δgp1–gp12:Nluc phage at the same location. This was done by using specified sets of primers to amplify the full PE3Δgp1–gp12 or PE3Δgp1–gp12:Nluc phage genome by PCR in overlapping segments as observed in **Figure 5**.

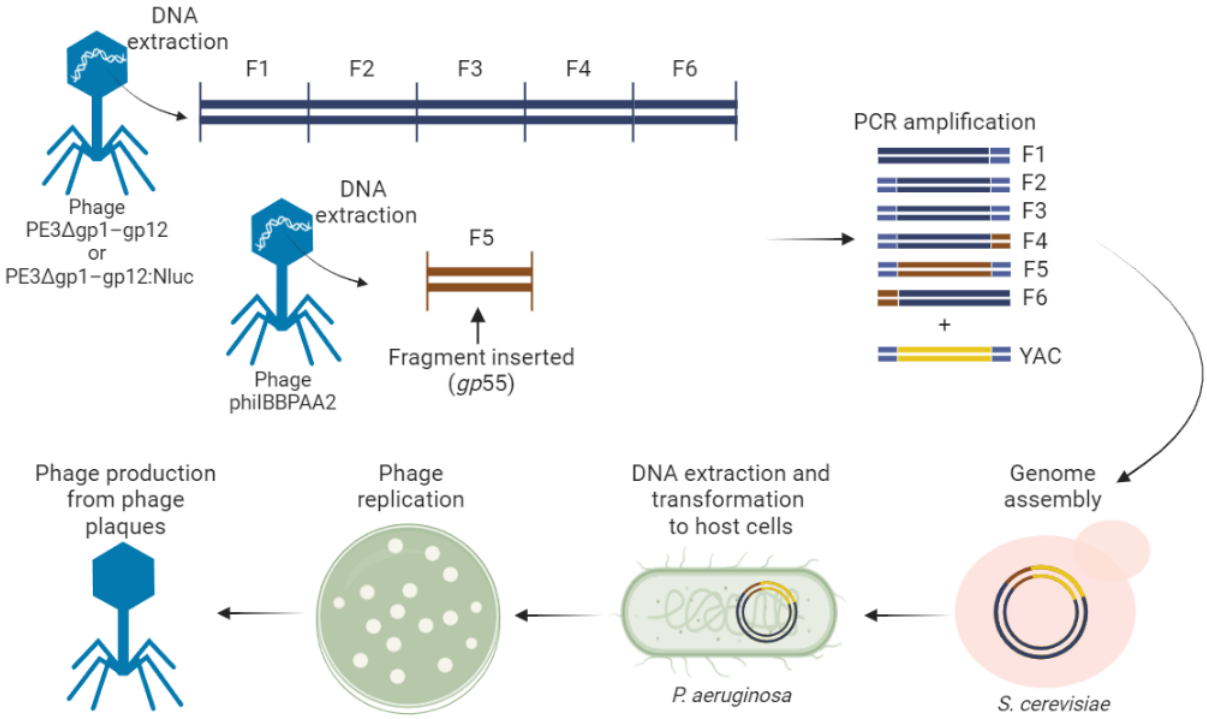

Figure 5 - Process for assembling chimeric phages. The whole phage genome is amplified in overlapping PCR products from phage DNA. The linearized YAC and PCR products are co-transformed into yeast cells where they are properly assembled in consequence of the overlapping regions. In order to recover infectious phage particles, the phage genome that was captured into the YAC is then extracted from yeast cells and transformed into the host *P. aeruginosa* cells.

2.5.1. Preparation of the PCR products for genome engineering

The preparation of PCR products for genome engineering was done using specific sets of primers (**Tables 10** and **11**), and the Phusion™ Plus DNA Polymerase (ThermoFisher Scientific) or the Xpert High Fidelity DNA Polymerase (Grisp) (**Tables 12** and **13**). After confirming the DNA amplification of all fragments by electrophoresis, the DNA Clean and Concentrator kit (Zymo Research) was used to purify and recover all the PCR fragments. In order to capture phage genomes into the yeast artificial chromosome (YAC) pRS415, homologous overhangs to the 5′ and 3′ ends of the phage genome were inserted in the primers used to amplify it. For each yeast transformation, seven PCR products were used, including the YAC (**Table 10**).

Table 10 – Backbone, transformations (T1 and T2) and the respective DNA fragments, template, size and primers used

Backbone	DNA fragment	Template	Size (bp)	Primers used for amplification
	YAC	pRS415	3041	P1/P2

Chimeric phage genome	DNA fragment	Template	Size (bp)	Primers used for amplification
T1	F1	PE3Δgp1–gp12 phage	8877	P3/P4
	F2	PE3 phage	8179	P5/P6
	F3	PE3 phage	8061	P7/P8
	F4	PE3 phage	10277	P9/P10
	F5	A2 phage	648	P11/P12
	F6	PE3 phage	5294	P13/P14
T2	F1	PE3Δgp1–gp12 phage	8877	P3/P4
	F2	PE3 phage	8179	P5/P6
	F3	PE3 phage	8061	P7/P8
	F4	PE3 phage	10277	P9/P10
	F5	A2 phage	648	P11/P12
	F7	PE3Δgp1–gp12:Nluc phage	5489	P13/P14

Table 11 - Primers used to amplify all the PCR products for the yeast transformation. Overhangs are underlined

Primer	Sequence (5'→3')
P1	CCTGTGGTCCTGTCGGGTGGTGCGGGAGTGGCTGGTGTCTCATGAGCGGATACATATTTGAATGT
P2	GCCTACGGGGGAAGGGTGGGCTGATCAGAGTCGGGCCTTGTTCATGTGTGTTCAAAAACGTTATA
P3	CCCGACTCTGATCAGCCCAC
P4	CAGCATCTTGATGCCGTCCAC
P5	CTGTTGAGTCATCAGACGTGGC
P6	CGATGAATCCGCTCTGGTAGC
P7	GCCATCGCAGGTCTGCTGG
P8	GTACTGGTGGCAGATCATCTCG
P9	GTCGCCGAAGACGTTACCAGC
P10	GTTAATATAAGTTGCGACCTCAAGACCCATAGGTTATGCCCTCGCCACC
P11	CTGGAGTTTACGGTGGCGAGGGCATAACCTATGGGTCTTGAGGTCGCAAC
P12	GGTCTGGGTTGAAGTCGTAGATCAGTGCCATCAGTTCTTAATGATGAAGAACACAG
P13	CTGTTCTGTGTTCTTCATCATTAAGAACTGATGGCACTGATCTACGACTTC

P14	CCAGCCACTCCCGCACCA

Table 12 - Components and quantities used for PCR with Xpert High Fidelity DNA Polymerase

Components	Concentration
Xpert HighFidelity DNA Polymerase (2U/µl)	0.02-0.04 U/µL
5× PCR Buffer	1×
Primers	0.4 µM
Template DNA	25 ng
Water, nuclease free	to 50 µL

Table 13 - Thermocycling conditions used for PCR with Xpert High Fidelity DNA Polymerase

Step	Temperature	Time
Initial Denaturation	95 °C	1 min
25-35 Cycles	95 °C	15 sec
	65 °C	15 sec
	72 °C	30 sec/Kb
Final Extension	72 °C	3 min
Hold	4 °C	

2.5.2. Genome engineering

The preparation of yeast competent cells was done according the procedure reported by Ando et al., (2015) with minor modifications. *S. cerevisiae* BY4741 was cultivated for roughly 20 hours at 30 °C, 250 rpm in 5 mL of YPD. This culture was diluted by adding 5 mL into 50 mL of YPD and incubated at 30 °C, 250 rpm for 5 hours. Following a centrifugation step (5000 ×g, RT, 5 min), the cells were collected, washed twice with 25 mL of water, and resuspended in 1 mL of sterile ddH_2O. After a second centrifugation (13000 ×g, RT, 30 sec), the cell suspension was resuspended in 1 mL of sterile ddH_2O. For each transformation, 100 µL of this cellular suspension were used.

All the phage DNA fragments and the linearized YAC were placed in a tube (200 ng of linearized pRS415 and 3:1 (insert:vector) of each DNA fragment) in 34 µL water, and then mixed with the transformation mixture (100 µL yeast competent cells, 240 µL 50 % (w/v) PEG 3350, 36 µL 1.0 M

Lithium Acetate, and 50 µL 2 mg/mL salmon sperm DNA). After 45 min of incubation at 42 °C, the mixture was centrifuged (13000 ×g, RT, 30 sec), resuspended in 1 mL of YPD and incubated at 30 °C for 2-3 hours with 120 rpm of agitation. The yeast transformants were then selected on synthetic defined medium with leucine dropout (SD-Leu) [0.67 % Yeast Nitogen Base (YNB), 0.069 % CSM-Leu, 2 % dextrose] agar plates incubated at 30 °C for 3 days.

After, yeast colony PCR was performed to confirm the correct assembly of the fragments. For this, randomly chosen colonies were resuspended in 10 µL of 0.02 M NaOH and heated at 99 °C for 10 min. The supernatant was then used as template for the PCR reaction with DreamTaq™ DNA polymerase (ThermoFisher Scientific) following the manufacturer's instructions (**Table 14**). The primers used in yeast colony PCR for both transformations are listed in **Table 15** and the PCR conditions are detailed in **Table 16.** All the PCR reactions were carried out in a DNA thermocycler (T100™ Thermal Cycler (BioRad)).

Table 14 - PCR mix components and concentrations for yeast colony PCR

Components	Concentration
DreamTaq™ Green PCR Master Mix (2×)	25 µL
Forward primer	0.5 µM
Reverse primer	0.5 µM
Template DNA	3 µL
Water, nuclease free	to 50 µL

Table 15 – Primers used in yeast colony PCR and their parameters. Tm represents the melting temperature

Primer	Sequence (5'→3')	Tm (°C)	GC content (%)
P15	Fw: GCACCTTCCGGCTGATCC	59	67
P16	Rv: GCAGAAGTCCAGCACGTCG	59	63

Table 16 - Thermocycling conditions for a yeast colony PCR

Step	Temperature	Time
Initial Denaturation	95 °C	3 min
30 Cycles	95 °C	30 sec

	55 °C	30 sec
	72 °C	1 min/Kb
Final Extension	72 °C	10 min
Hold	4 °C	

The PCR products from yeast colony PCRs were run on a 1 % (w/v) agarose gel. The positive transformants that showed the correct assembly were inoculated in SD-Leu liquid medium for 24 h at 30 °C. Then, the YAC-Phage DNA was extracted from yeast cells using the QIAprep Spin Miniprep Kit (Qiagen) combined with zymolyase® 20T (Grisp) following a previously described protocol (Ando et al., 2015) and the DNA concentration was determined using the NanoDrop™ One Microvolume UV-Vis Spectrophotometer (ThermoFisher Scientific).

2.5.3. Transformation of captured phage genome into *P. aeruginosa* cells

The preparation of electrocompetent *P. aeruginosa* PAO1 cells was performed according to a method previously described by Choi et al., (2006) with minor modifications. Briefly, 6 mL of an overnight-grown culture were distributed by 4 microcentrifuge tubes and centrifuged (16000 ×g, RT, 1 min). Each pellet was then washed twice with 1 mL of 300 mM sucrose. For each transformation, the 4 bacterial pellets were resuspended in a total of 100 µL of 300 mM sucrose and mixed with the extracted DNA (YAC-phage DNA) (Pires et al., 2021). This mixture was then transferred into a 2 mm gap electroporation cuvette, a pulse (25 µF, 200 Ω, 2.5 kV) was applied using an *E. coli* Pulser™ Transformation Apparatus (BioRad) and 900 µL of LB medium was added to recover the cells. Before performing plaque formation experiments, the cellular suspension was transferred to a tube and incubated at 37 °C for 2-4 hours with 120 rpm of agitation (Pires et al., 2021).

About 300 µL of the cellular suspension produced by YAC-phage DNA electroporation were combined with 3 mL of LB soft agar and plated in LBA plate in order to recover the chimeric phages. The plates were examined to see if any phage plaques were present after overnight incubation at 37 °C (Pires et al., 2021).

2.5.4. Phage production and sequencing

When phage plaques were recovered after the electroporation of the YAC-phage DNA, the recombinant phages were then propagated to high titers. Briefly, a single phage plaque was picked and eluted in 50 µL of SM buffer. Then, this solution was used to infect 15 mL of a *P. aeruginosa* PAO1 log-phase culture. After incubation for 8 h at 37 °C, this suspension was centrifuged (9000 ×g, 4 °C, 10 min) and the supernatant was collected, filtered (0.22 µm) and kept at 4 °C until further use (Pires et al., 2017).

Finally, the phage titre was evaluated by PFU's counting. The phage stock solution was serially diluted in SM buffer and 10 µL of each dilution were plated into the bacterial lawns. The plates were incubated overnight at 37 °C and the PFU's were then counted.

The correct insertion of the gene encoding the TFP on the chimeric phages was confirmed by PCR, with the primers used on yeast colony PCR and after product cleaning, by Sanger sequencing.

2.5.5. Host-range of the chimeric phages

The host-range of the chimeric phages was evaluated against the clinical strains of *P. aeruginosa* to compare to the wild-type phage. This was performed as described in section 2.3. In the cases where lysis was seen, phage suspensions were serially diluted and the dilutions were plated on the bacterial lawns to look for potential cases of lysis from without.

Chapter 3

RESULTS AND DISCUSSION

3. RESULTS AND DISCUSSION

3.1. Fast and sensitive detection of *P. aeruginosa* using reporter phages

Rapid and sensitive methods are highly needed for the specific detection of *P. aeruginosa,* namely in clinical settings. An accurate identification of the pathogen allows a rapid implementation of the appropriate treatment, reducing the severity of infection and also the associated costs. The PE3Δgp1–gp12:Nluc reporter phage carrying the Nluc gene was previously assembled using the yeast-based phage-engineering platform at the research group and here, this phage was explored to assess its sensitivity and specificity to detect *P. aeruginosa* cells and evaluate the detection limit.

The sensitivity of this reporter phage system was quantified by infecting serial dilutions of host cells with the phage at 10^5 PFU/mL and quantifying the light-emitting RLUs (Relative light units) for 7 h. **Figure 6** shows the dispersion graph referring to the RLUs over time, for assays without enrichment.

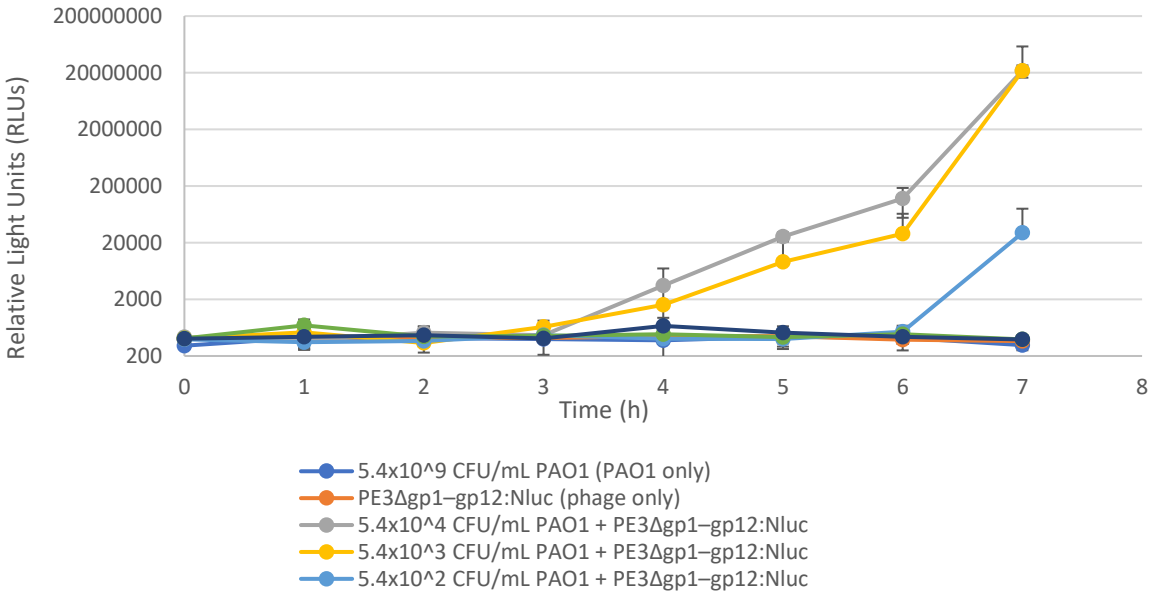

Figure 6 - Relative light units (RLUs) over time, without sample enrichment. Error bars represent standard deviations from 3 independent experiments.

The bar graph referring to the RLUs over time, for assays without enrichment, is represented in **Figure 7**.

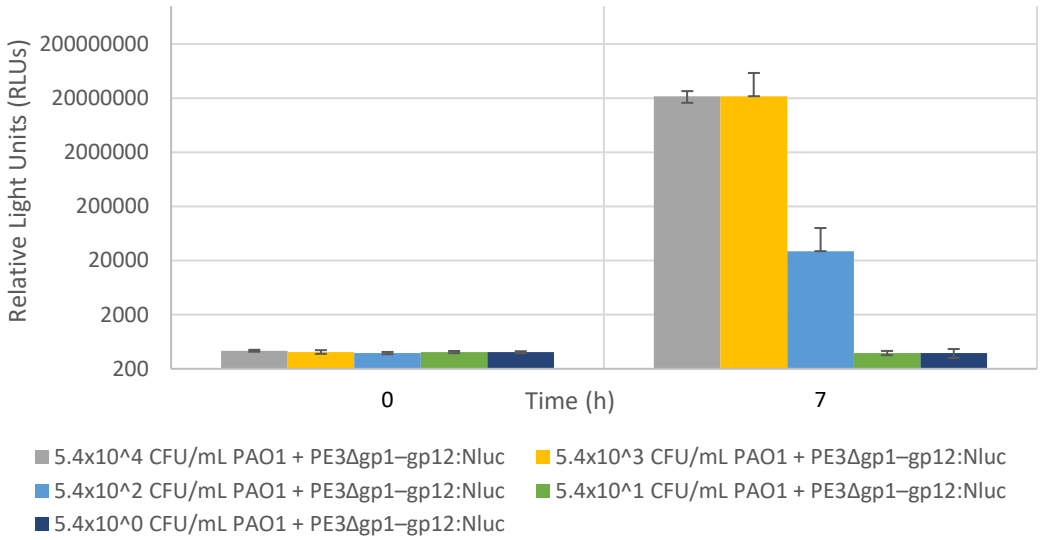

Figure 7 - Graphic representation of bars corresponding to different concentrations of bacteria infected with the reporter phage, without sample enrichment, of relative light units at time 0 h and 7 h. Error bars represent standard deviations from 3 independent experiments.

According to the results from Figure 7, the detection limit of phage PE3Δgp1–gp12:Nluc was 5.4×10^{2} CFU/mL but to try to improve this limit of detection, an additional test was carried out. *P. aeruginosa* PAO1 was enriched before phage addition by incubating the bacterial dilutions at 37 °C for 3 h. After adding the phage, the infection was tracked for 4 h in order to keep the total time of the experiment 7 h, similarly to the assays without enrichment. The results obtained for the dispersion graph referring to the RLUs over time, for assays with enrichment are represented in **Figure 8**.

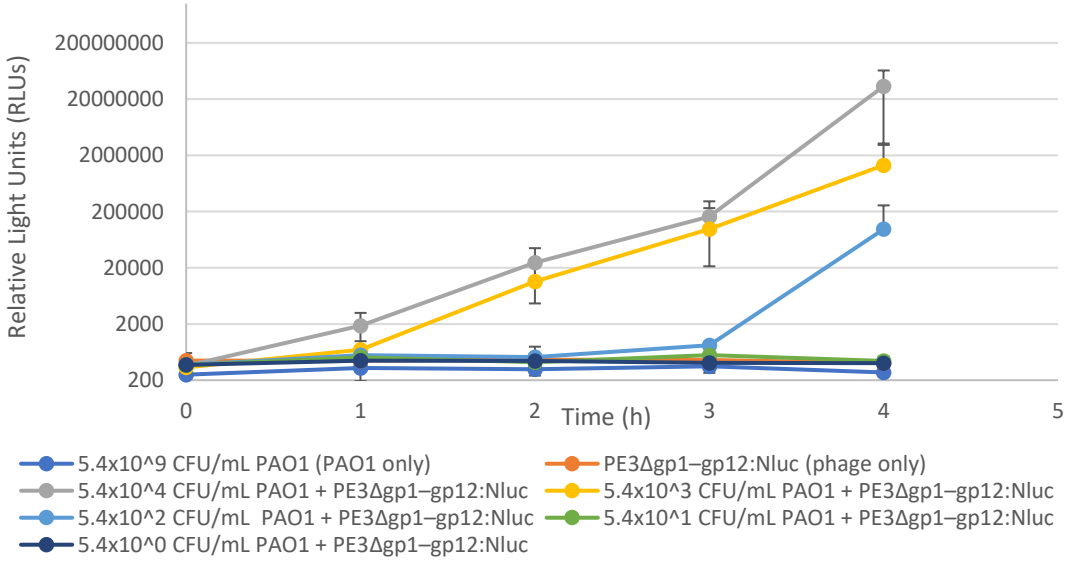

Figure 8 - Relative light units (RLUs) over time, with sample enrichment. Error bars represent standard deviations from 3 independent experiments.

The bar graph referring to the RLUs over time, for assays with enrichment, is represented in **Figure 9**.

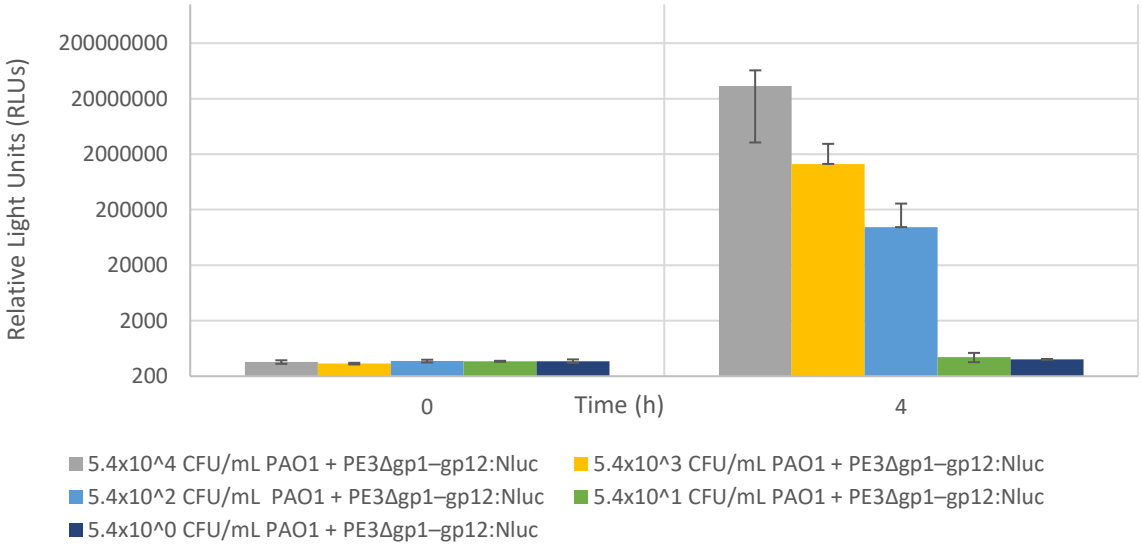

Figure 9 - Graphic representation of bars, corresponding to different concentrations of bacteria infected with the reporter phage, with enrichment, of relative light units over time. Error bars represent standard deviations from 3 independent experiments.

The detection limit is defined as the minimum number of bacteria needed to produce a signal that is distinguishable from the background. The minimum CFU number detectable by the PE3Δgp1–gp12:Nluc phage was 540 per mL for both experiments (with and without enrichment). Although the enrichment step of 3 h led to a higher luminescence signal without compromising the total time of the method, the limit of detection was the same and thus, this step can be skipped as the protocol without enrichment is simpler and easier to perform. Based on this, all the subsequent experiments were performed without the enrichment step. Detection assays with the reporter phage were optimized and repeated in triplicate for the host strain PAO1 and the results measured after 7 h are represented in **Figure 10**.

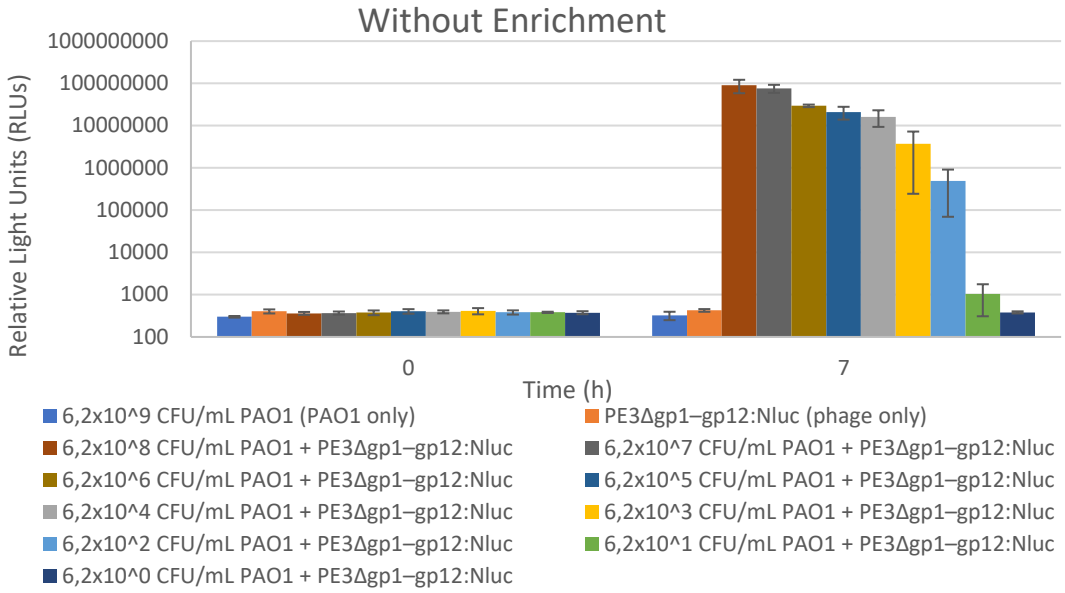

Figure 10 - Bioluminescence output (RLUs) of serial dilutions of host strain infected with the reporter phage PE3gp1-gp12:Nluc with 10^5 PFU/mL and respective controls. Error bars represent standard deviations from 3 independent experiments.

According to Figure 10, it is possible to observe that the PE3Δgp1–gp12:Nluc reporter phage reliably detects 620 CFU/mL of the host strain. This was accomplished within 7 hours, which is 41 hours less time than the conventional selective plating techniques (Tramper-stranders et al., 2005).

Currently, reporter phages are mostly focused on the food industry. To build a reporter phage for the detection and differentiation of live *Listeria* cells, which cause a serious foodborne illness, Meile et al., (2020) used CRISPR-Cas-assisted phage editing. In less than 24 hours, the NLuc-based phage, A511::nlucCPS, can identify one CFU of *L. monocytogenes* in 25 g of artificially contaminated milk, cold cuts, and lettuce. More recently, Erickson et al., (2021) used homologous recombination to create a recombinant form of LPJP1 that encodes the NanoLuc luciferase. Within four hours, this luciferase reporter phage detected 100 stationary phase colony forming units of both *L. grayi* subspecies.

Hinkley et al., (2018) genetically altered a T7 coliphage to express NanoLuc using homologous recombination and the use of microcrystalline cellulose to concentrate the fusion reporter was then shown to enable the detection of a maximum of 10 CFU/mL *E. coli* within three hours. Also, the limit of detection for the reporter phages created by Nguyen et al., (2020) using homologous recombination was 10-100 CFU per mL in *Salmonella* culture within two hours. In food matrix tests, a combination of engineered phages successfully identified 1 CFU in either 100 g of powdered infant formula with a 16 h enrichment or 25 g of ground turkey with a 7 h enrichment.

Here, as the phage is specific for *P. aeruginosa* species, clinical isolates known to be sensitive to phage PE3Δgp1–gp12:Nluc were also tested (strains 5, 6, 16, 21, 23, 27 A65, 065 and 092) to assess the detection limit in other bacterial strains rather than the host. Beyond that, the methodology was also repeated for clinical strains of *E. coli* (A51), *Klebsiella pneumoniae* (A36 and A57), *Staphylococcus aureus* (A1, A9 and A39), *Enterococcus faecalis*, *Enterococcus faecium* (A74 and A78 respectively) and *P. aeruginosa* PA14.

The **Figure 11** shows the RLUs emitted after seven hours of phage infection of each bacterial strain above mentioned.

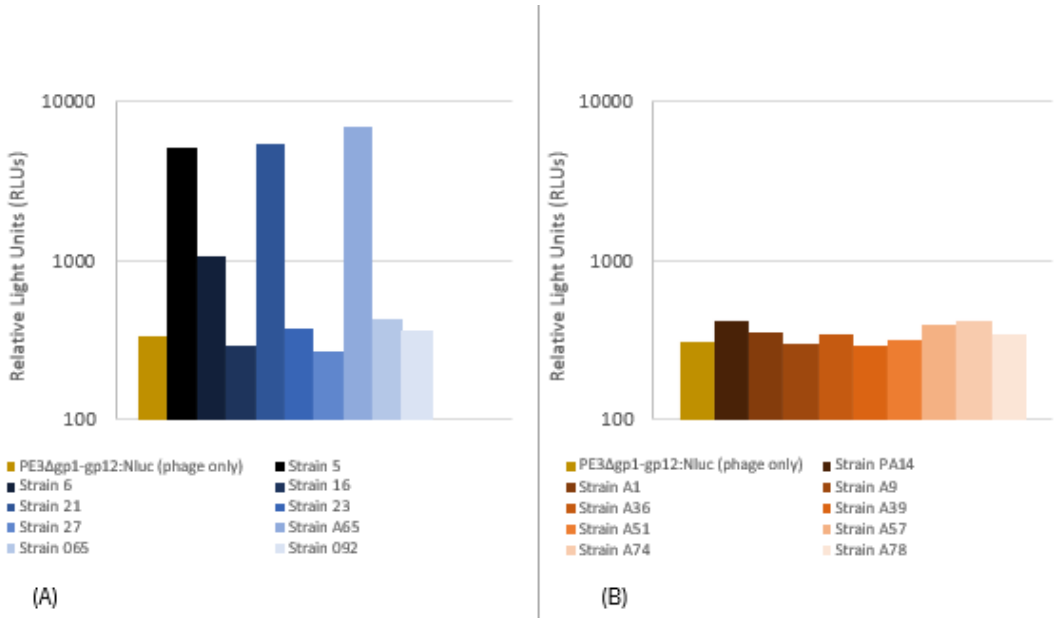

Figure 11 - Bioluminescence output (RLUs) of different clinical strains infected with PE3Δgp1-gp12:Nluc phage (10^5 PFU/mL) for 7 h . (A) *P. aeruginosa* strains that are sensitive to phage; (B) clinical strains that are not infected by the phage (chosen as negative controls).

As observed in Figure 11 (A), phage PE3Δgp1-gp12:Nluc was unable to detect five (16, 23, 27, 065 and 092) out of the nine clinical strains of *P. aeruginosa*. All these 9 strains are sensitive to the phage, which was observed though determination of the lytic spectra and EOP (**Table 17**). This is unexpected, according to EOP results most phage—bacterium combination was classified as a medium production and therefore, all strains were supposed to be detected. Since this phage is specific for *P. aeruginosa*, as expected, all other species tested did not show any luminescence, and in this case there were no false positives, as can be seen in Figure 11 (B). Among the 4 clinical strains that the reporter phage was capable to detect, the detection limit is represented in **Figure 12**.

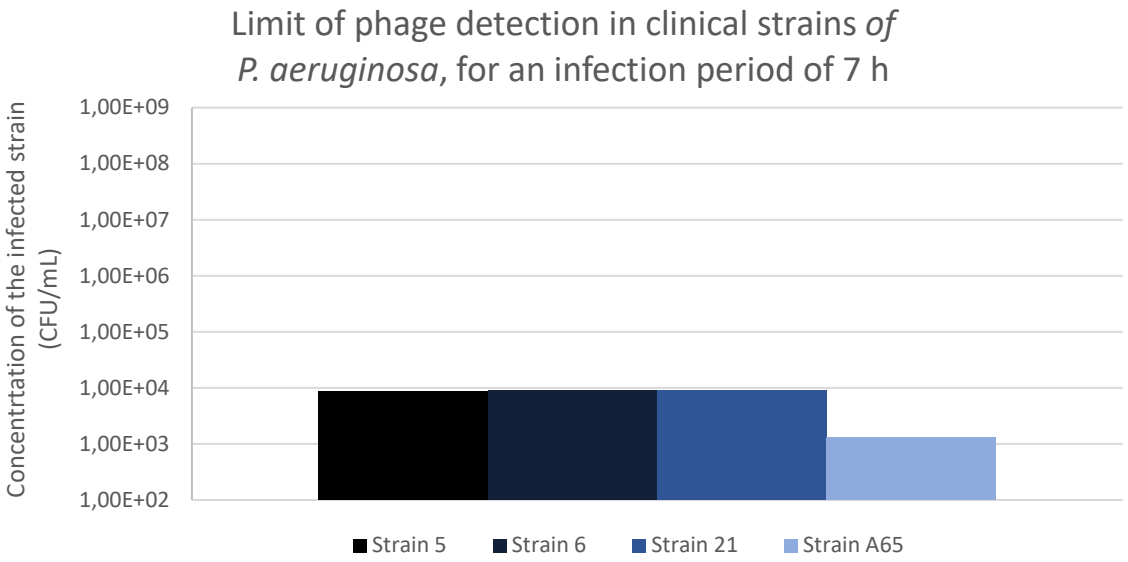

Figure 12 – Concentration (CFU/mL) of artificially infected samples. Samples were incubated with 10^3 PFU/mL of PE3gp1-gp12:Nluc phage.

The minimum CFU number detectable by the PE3Δgp1–gp12:Nluc phage for those strains is in the range of 10^3 CFU per mL, which is approximately ten times higher than the minimum concentration obtained for the host strain PAO1. It would be interesting to test the phage in more clinical strains rather than just a few, as this severely restricts the ability to make reliable conclusions about this technique. The subsequent stage will also involve running these detection assays in real samples from patients like blood, urine, or other fluids.

In conclusion, the *P. aeruginosa* reporter phage was capable of reliably detect 620 CFU in 1 mL of samples contaminated with PAO1 in less than 8 h, thus overcoming the major limitation of the currently used detection methods, which is time-consuming. On the other hand, this technique was not capable of detecting all the strains known to be sensitive to the phage, which is an issue. This implies, and hence supports, the requirement of phage-engineering work to expand the host range of the phage and a possible approach may be the cloning of additional TFPs from other phages with complementary host ranges.

3.2. Determination of the host range and efficiency of plating

Seven phages (PE1, A2, DP1, PA14G, PA14-20, PE3 and PE3Δgp1–gp12:Nluc) were tested against a panel of 52 *P. aeruginosa* clinical strains by spot test in order to evaluate the lytic spectra of each phage. **Table 17** shows the host range of each phage, where LFW means lysis from without. This is

a bacterial lysis caused by phage adsorption without phage production, which is induced by high multiplicities of infection (typically 100 times more phages than bacteria) (Abedon, 2011; Mirzaei & Nilsson, 2015). According to the results from Table 17, only the *P. aeruginosa* strains 2, 10, 14, A63 and 149 were not lysed by any of the studied phages.

Table 17 - EOP of phages against different strains of *P. aeruginosa*

Phage Strain	PE1	A2	DP1	PA14G	PA14-20	PE3	PE3Δgp1–gp12:Nluc
1	0.4	0.5	0.9	-	0.2	-	-
2	-	-	-	-	-	-	-
3	0.002	<0.001	-	-	0.3	-	-
4	0.043	LFW	LFW	-	0.020	-	-
5	0.1	0.4	0.016	0.001	0.3	0.3	0.4
6	0.1	0.4	0.8	0.1	0.2	0.6	0.4
7	0.017	<0.001	-	-	0.5	-	-
8	LFW	LFW	LFW	<0.001	0.5	LFW	LFW
9	-	LFW	LFW	LFW	LFW	-	-
10	-	-	-	-	-	-	-
11	-	-	-	0.1	LFW	0.3	LFW
12	0.006	LFW	-	<0.001	LFW	0.3	LFW
14	-	-	-	-	-	-	-
15	-	LFW	LFW	-	LFW	-	-
16	LFW	0.1	0.004	0.1	0.1	0.3	0.4
17	0.1	-	-	0.031	0.020	0.1	LFW
18	LFW	0.005	LFW	-	LFW	-	-
19	LFW	-	-	<0.001	0.020	-	-
20	0.2	0.006	-	-	0.4	LFW	-
21	0.2	0.4	0.029	<0.001	0.5	0.3	0.004
22	0.3	0.1	-	-	0.3	-	-
23	0.1	LFW	-	0.003	0.4	0.3	0.8

24	0.040	-	-	-	0.4	-	-
25	0.2	0.5	0.9	-	0.4	-	-
26	0.1	-	-	LFW	0.5	LFW	LFW
27	0.4	0.1	1.0	0.5	0.2	0.4	0.040
28	0.1	0.2	0.8	LFW	0.2	<0.001	LFW
29	0.022	0.1	0.4	LFW	0.2	LFW	LFW
A22	0.1	0.2	1.0	0.5	0.2	LFW	LFW
A63	-	-	-	-	-	-	-
A64	-	LFW	LFW	0.0	LFW	LFW	LFW
A65	LFW	LFW	-	0.5	LFW	0.2	0.4
A66	0.3	LFW	-	0.5	0.2	LFW	LFW
A67	-	LFW	LFW	0.004	LFW	LFW	LFW
A69	-	LFW	-	0.5	LFW	0.3	LFW
A70	0.2	0.8	1.0	-	0.4	-	-
A71	-	LFW	LFW	-	LFW	-	-
052EX	<0.001	-	-	-	LFW	LFW	LFW
O64	0.010	LFW	<0.001	-	0.2	-	-
O65	-	-	-	0.4	LFW	0.004	0.4
O77	0.020	LFW	0.1	-	0.2	-	-
O78	-	0.2	<0.001	0.6	LFW	0.2	LFW
O79	0.2	0.2	0.9	LFW	0.2	LFW	LFW
O92	-	-	-	0.3	LFW	0.1	0.020
144	0.1	0.5	0.1	0.3	0.2	0.5	LFW
149	-	-	-	-	-	-	-
wzy	-	LFW	LFW	0.3	LFW	0.4	0.1
wbpL	LFW	-	LFW	<0.001	LFW	0.1	0.007
rmlC	-	-	LFW	-	LFW	-	-
rmd	0.3	0.1	0.1	<0.001	0.8	0.5	0.6
PAO1	1.0	1.0	1.0	1.0	1.0	1.0	1.0

PA14	0.4	-	-	0.3	0.8	-	-
% infection	56	40	35	50	58	38	25
% high productive infection	2	10	15	13	13	8	6

When the productive infection on the target bacteria produced at least 50 % of the PFU reported for the primary host, the average EOP value (average PFU on target bacteria / average PFU on host bacteria) for a certain phage—bacterium combination was classified as "High production". EOP values between 0.001 and 0.1 were categorized as "Low production" efficiency, while values greater than 0.1 but less than 0.5 were classified as "Medium production" efficiency. An EOP of 0.001 or less was considered inefficient (Mirzaei & Nilsson, 2015; Viazis et al., 2011).

As expected, the spot test assays revealed different host ranges for each phage. While the PA14-20 phage was able to infect almost 58 % (30 strains) of the 52 strains tested, the phage PE3Δgp1–gp12:Nluc could only lyse 25 % (13 strains) of the 52 strains. The percentage of strains where high productive infection (EOP≥0.5) was achieved ranged from 13 %, or 7 out of the 52 strains, for the PA14-20 phage, to 6 % (3 strains) for the PE3Δgp6–gp12:Nluc phage, which was significantly lower than the findings of the spot tests.

After analyzing the results, a broader and complementary host range was found between phages A2 and PE3 and were therefore selected for the functional analysis of TFPs.

3.3. Cloning and functional analysis of potential TFPs

The two phages (A2 and PE3) selected for this task were previously isolated and characterized (Pires et al., 2014). Although already sequenced and annotated, a deeper genome analysis was done here to screen for potential TFPs (**Supplementary material – Table S3** and **Table S4**). After a manual analysis of the genome of each phage, two potential TFPs were identified and studied for phage A2 and five potential TFPs for phage PE3. In phage A2, these TFPs are encoded by genes 53 and 55 (nucleotide and aminoacid sequence available in **Supplementary material – Table S2**), and in phage PE3 they are encoded by genes 39, 44, 45, 46 and 47 (nucleotide and aminoacid sequence available in **Supplementary material – Table S2**). These proteins were selected for cloning into the pGFP plasmid, expression,

purification and subsequent functional analysis by epifluorescence microscopy. The annotated genomic map of phage A2 is shown in **Figure 13**.

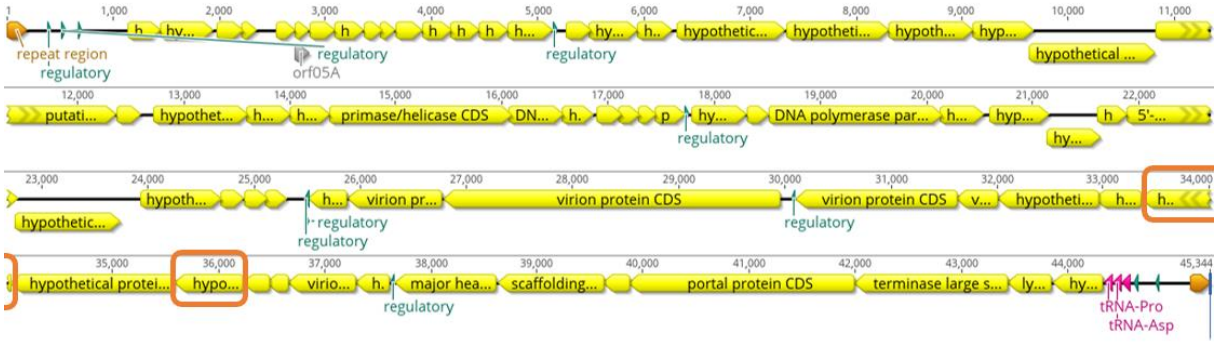

Figure 13 - Genome map of *P. aeruginosa* phage philBB-PAA2 using Geneious Prime. The regions highlighted in red represent the genes that encode TFPs.

The annotated genomic map of phage PE32 is shown in **Figure 14**.

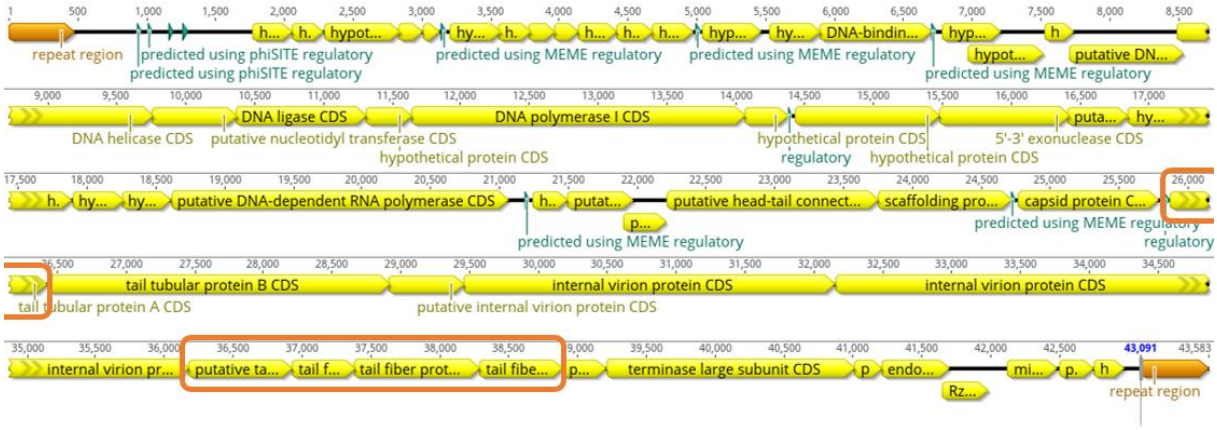

Figure 14 - Genome map of *P. aeruginosa* phage vB_PaeP-PE3 using Geneious Prime. The regions highlighted in red represent the genes that encode TFPs.

The amplification of the previously mentioned tail fiber genes from phages A2 and PE3 was confirmed on a 1 % (w/v) agarose gel and the results are shown in **Figure 15**. A temperature gradient was created to determine the ideal annealing temperature, and the optimized conditions were selected.

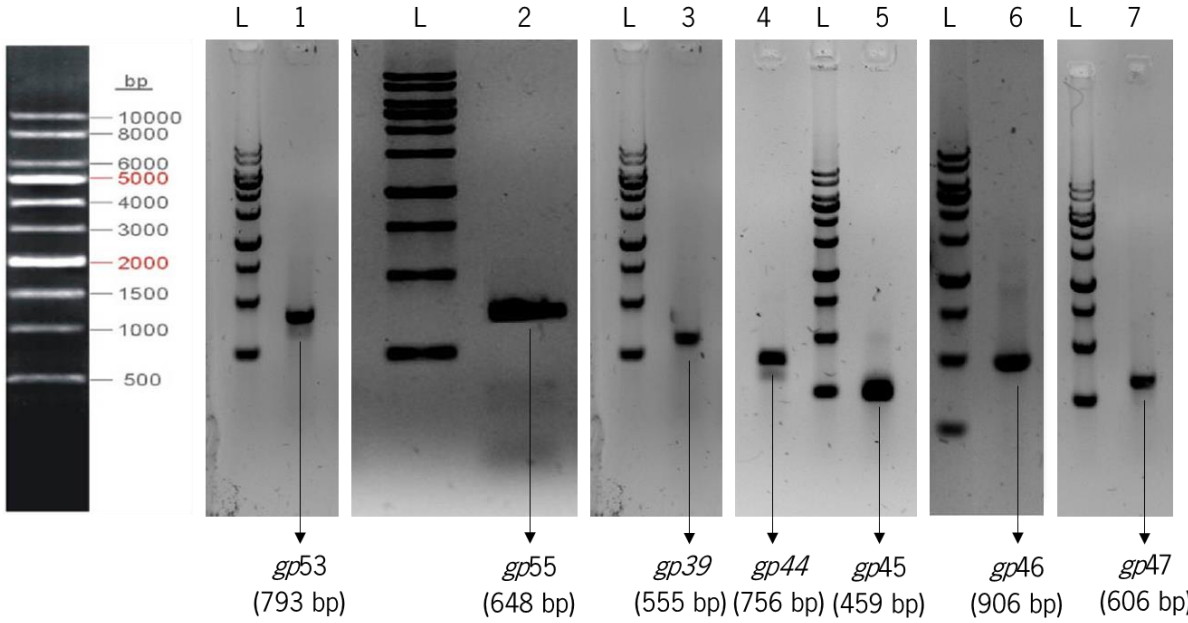

Figure 15 - Gel electrophoresis with results from the PCR amplification of the following genes: (1) *gp*53 from A2 (annealing temperature: 55 °C); (2) *gp*55 from A2 (annealing temperature: 55 °C), (3) *gp*39 from PE3 (annealing temperature: 60 °C), (4) *gp*44 from PE3 (annealing temperature: 55 °C), (5) *gp*45 from PE3 (annealing temperature: 55 °C), (6) *gp*46 from PE3 (annealing temperature: 60 °C), (7) *gp*47 from PE3 (annealing temperature: 55 °C) and (L) 1 Kb GRS Ladder DNA (Grisp). The sequence length is expressed in bp.

For all PCR products, the gels revealed the presence of a single band of the expected size and no secondary bands were observed, confirming the correct amplification of the genes without unspecific amplification fragments.

After digesting and cleaning the PCR products, the putative genes encoding TFPs were cloned into the pGFP plasmid, resulting in the recombinant plasmids: pGFP_A2gp53, pGFP_A2gp55, pGFP_PE3gp39, pGFP_PE3gp44, pGFP_PE3gp45, pGFP_PE3gp46 and pGFP_PE3gp47.

The constructed plasmids were transformed by heat shock into competent *E. coli* AE (DE3) cells, and the resulting colonies were randomly selected and subjected to colony PCR to assess gene insertion into the plasmid. The products of each colony PCR were visualized on a 1 % (w/v) electrophoresis agarose gel, as shown in **Figure 16**.

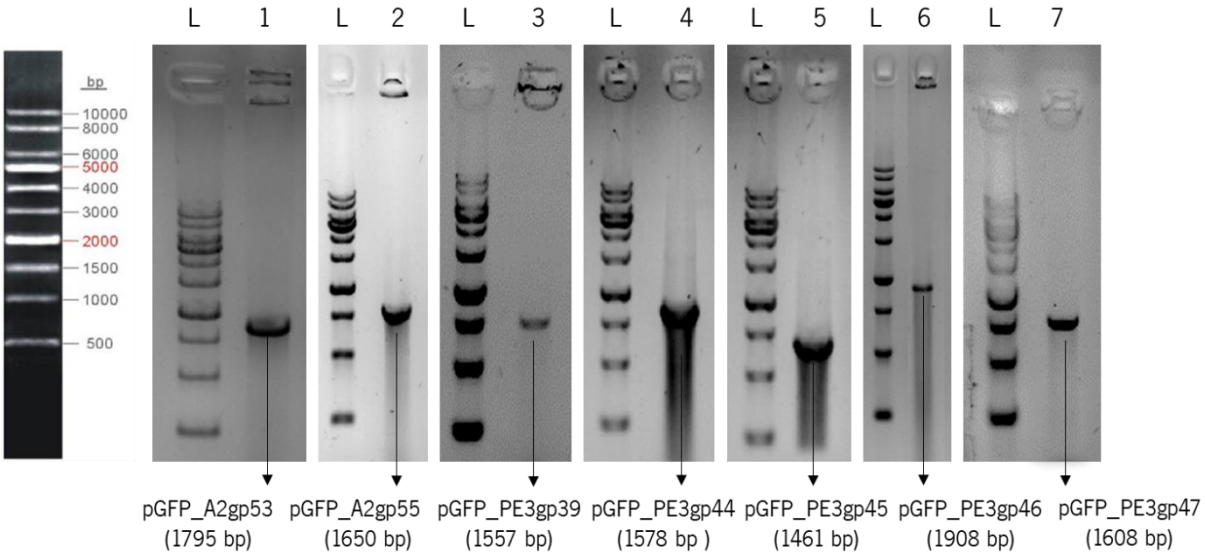

Figure 16 - Gel electrophoresis showing the amplification of one correct transformant for each gene. (1) pGFP_A2gp53 AE, (2) pGFP_A2gp55 AE, (3) pGFP_PE3gp39 AE, (4) pGFP_PE3gp44 AE, (5) pGFP_PE3gp45 AE, (6) pGFP_PE3gp46 AE, (7) pGFP_PE3gp47 AE and (L) 1 Kb GRS Ladder DNA (Grisp). The DNA sizes presented include the size of TFPs amplification, plus an additional 1002 bp correspondent to the amplification of the aceGFP gene and of a short sequence of the plasmid.

The pGFP plasmid has 1002 bp (corresponding to the GFP gene and an additional sequence form the pET28a(+)) and therefore, even empty plasmids will produce an amplification product using the T7 primers, which work as a negative control of the colony PCR. Figure 16 shows a 1 % (w/v) agarose gel electrophoresis with bands with the correct size of amplification for each construct, confirming the correct transformation of the plasmids under study. Clones with the expected band were selected and the plasmid extracted and sent for Sanger sequencing in order to confirm the correct insertion of the gene.

After confirming the correct insertion of each target gene, the following step was the heterologous expression of the proteins. A small-scale expression test (50 mL) was performed to analyze the expression and solubility of the recombinant proteins and perform the functional analysis of the proteins under study. *E. coli* Arctic Express (DE3) expresses two cold-adapted chaperonins Cpn10 and Cpn60 from *Oleispira antarctica*, that assist in refolding of proteins (Agilent Technologies, 2015). The small-scale expression tests of all proteins showed that most of them were expressed in the soluble form and only the pGFP_PE3gp45 remained accumulated in the insoluble fraction. This fraction was resuspended and sonicated to exclude that the prevalence of insoluble protein was due to insufficient lysis and the amount of protein in the soluble portion was sufficient to carry out the subsequent experiments.

After affinity chromatography with NI^{2+}-NTA resin, purification of the fused proteins was confirmed through SDS-PAGE and a functional analysis of the TFPs by epifluorescence was conducted.

The results obtained from the SDS-PAGE gel are shown in **Figure 17.**

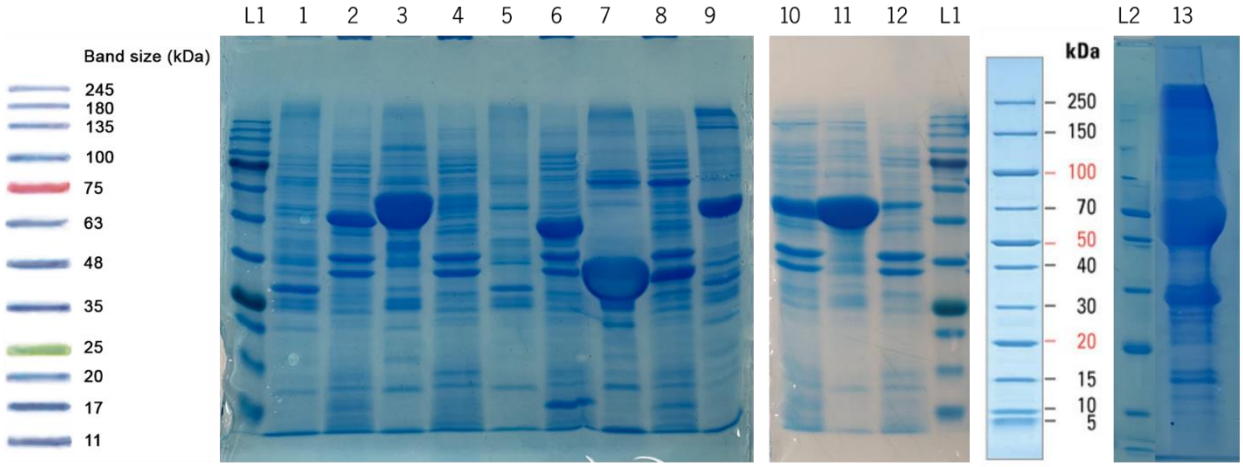

Figure 17 - SDS-PAGE with results of the purified proteins, expressed in AE cells. (1) pGFP_PE3gp39 1st elution, (2) pGFP_PE3gp39 pellet, (3) pGFP_PE3gp44 1st elution, (4) pGFP_PE3gp44 pellet, (5) pGFP_PE3gp45 1st elution, (6) pGFP_PE3gp45 pellet, (7) pGFP_PE3gp46 1st elution, (8) pGFP_PE3gp46 pellet, (9) pGFP_PE3gp47 1st elution, (10) pGFP_PE3gp47 pellet, (11) pGFP_A2gp53 1st elution, (12) pGFP_A2gp53 pellet, (L1) NZYColour Protein Marker II (Nzytech), (13) pGFP_A2gp55 1st elution and (L2) PageRuler™ Broad Range Unstained Protein Ladder The molecular weight is expressed in KDa.

In addition to TFP expression by SDS-PAGE, the expression was also detectable by the colour of the cultures after expression, which showed strong green staining due to the presence of the aceGFP fusion protein.

All the proteins transformed in AE (DE3) cells were shown to have the expected size but the pGFP_PE3gp46 protein showed a larger band close to 27 KDa, corresponding to aceGFP expression. This may indicate that some processing of the recombinant protein may have occurred, with cleavage of the fused protein. In cases where a stronger band appears in the pellet of the purified protein, a solubilization of the pellet was performed for further analysis. The presence of insoluble protein is typically caused by improper protein folding, which causes the protein to become inactive and expressed in inclusion bodies (Agilent Technologies, 2015). The pelleted protein was washed using a buffer containing the surfactant Triton X-100 and then protein was solubilized using urea. Although it was possible to solubilize the proteins, on the day after, the protein lost stability and precipitated again.

Then, a functional analysis of the TFPs was performed by epifluorescence. The amount of protein elution to be used in each reaction was estimated through the intensity of the colour (green) of the elution and the results of SDS-PAGE analysis of the expression. After observation under the microscope, protein pGFP_A2gp55 was the only one that demonstrated binding ability to *P. aeruginosa* PAO1 cells (**Figure 18**).

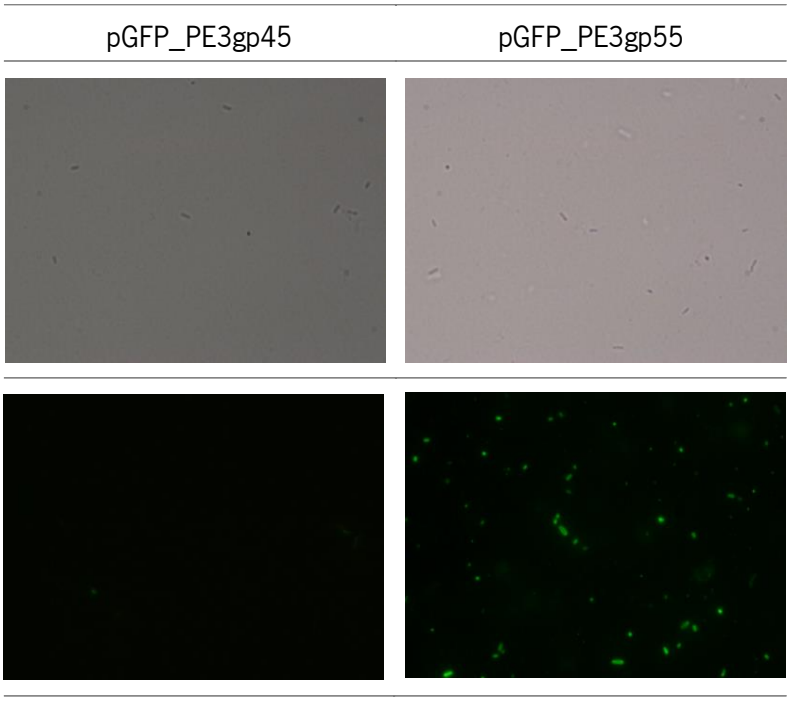

Figure 18 - Fluorescence microscopy assays for protein function analysis. On the first row, it is possible to observe the images without a filter and in the second, with the FITC filter, sensitive to green fluorescence. A negative example is shown in the first column, such as the pGFP_PE3gp45 protein and in the second column the only expressed protein that was able to bind *P. aeruginosa* PAO1, pGFP_PE3gp55.

Even though the remaining proteins were well expressed and showed a green, fluorescent colour, they were not able to bind to bacterial cells. After that, the expression of the proteins was repeated in different cells. *E. coli* C43 (DE3) contains genetic mutations that reduces the activity of T7 RNA Polymerase, thus preventing cell death by overexpression of recombinant toxic protein (Lucigen Corporation, 2018) and the *E. coli* BL21 (DE3) contains several genetic mutations and is widely used in order to obtain high yields of protein production. However, despite being well expressed, none of them showed binding capacity to *P. aeruginosa* PAO1, besides pGFP_A2gp55 protein.

There are different reasons to explain that. An incorrect folding of the protein may result in an inadequate exposure of the protein domain responsible for host recognition or even in a non-functional receptor binding protein. Moreover, it is possible that these proteins require the presence of other phage proteins to acquire the functional structure (usually trimerization) (North et al., 2019). Another hypothesis is that the proteins under study are not truly host recognition or binding proteins, even knowing that they are homolog to other identified receptor binding proteins in the NCBI database. The fact is that the majority of annotated phage receptor binding proteins deposited in the NCBI database were not validated

through functional assays and thus, they might not be able to recognize and bind to the phage bacterial hosts, leading to an erroneous selection of receptor binding proteins.

Considering the experimentally validated ability of pGFP_A2gp55 to bind PAO1 cells, homologous proteins were searched for cloning with the intention of performing a gene exchange between phages A2 and PE3, but none it was found. This impaired swapping homologous genes, but still enabled the addition of this protein to phage PE3 in order to express an additional receptor binding protein that could expand its host range.

3.4. Expanding the host range of *P. aeruginosa* phages by genome engineering

According to the fluorescence microscopy assays, only pGFP_A2gp55 protein was binding to the host cells, which corresponds to *gp*55 from A2 phage. Therefore, this gene was selected to be cloned between *gp*46 and *gp*47 genes from PE3 phage that also encode TFPs. Since the addition of new genes may require extra space in phage genomes, the phage PE3Δgp1–gp12 was used here as template for the introduction of the new gene as this phage is a variant of phage PE3 with a reduced genome and was previously shown to be functional and to have similar efficacy against the host cells (Pires et al., 2021).

The assembly of the new chimeric phage was accomplished using the yeast-based phage-engineering platform, which has been already used to efficiently manipulate the genomes of *E. coli*, Klebsiella and *P. aeruginosa* phages (Ando et al., 2015; Pires et al., 2021). In *S. cerevisiae*, homologous recombination is particularly effective due to the native gap repair system that facilitates the assembly of DNA fragments that share short homology regions, and phage genomes may be kept stable and are not hazardous to yeast. Since this method involves removing the phage genome from yeast and introducing it into the bacterial host to generate functional phage particles, its efficacy is constrained by the rate at which bacteria may undergo transformation (Pires et al., 2016).

In this work, 2 different constructs were tried: i) cloning of TFP in phage PE3Δgp1–gp12 without Nluc gene (transformation 1 - T1); and ii) cloning of TFP in phage PE3Δgp1–gp12:Nluc (transformation 2 - T2).

To assemble the chimeric phages, the entire phage genome of PE3Δgp1–gp12 phage was amplified by PCR in overlapping fragments using specific sets of primers (**Table 10**). For each transformation, seven PCR products spanning the phage genome, the gene gp55 from phage A2 to be cloned and the linearized YAC carrying homologous "arms" with the extremities of phage genome were

transformed into yeast cells where the recombination occurs because of the gap repair system that connects each fragment to the subsequent, resulting in a full phage genome captured in the YAC.The PCR amplification of all the DNA fragments was confirmed on a 1 % (w/v) agarose gel and the results are shown in **Figure 19**.

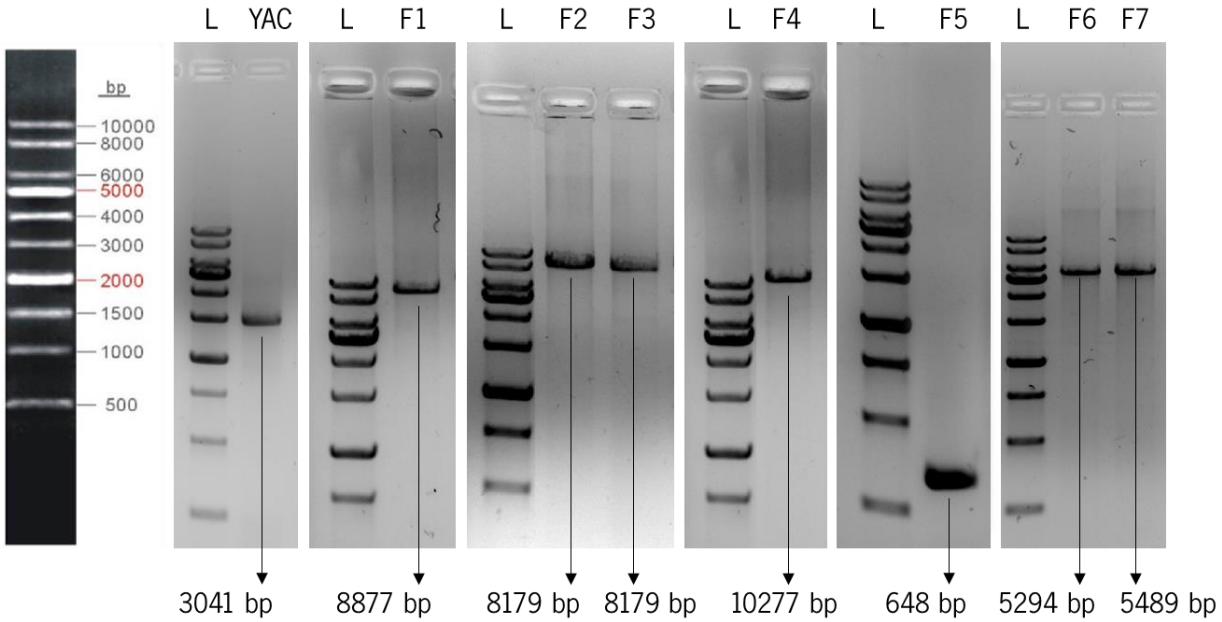

Figure 19 - Gel electrophoresis with results of the PCR amplification of each fragment. (YAC) annealing temperature: 65 °C; (F1) annealing temperature: 60 °C; (F2) annealing temperature: 60 °C; (F3) annealing temperature: 60 °C; (F4) annealing temperature: 60 °C; (F5) annealing temperature: 60 °C; (F6) annealing temperature: 65 °C; (F7) annealing temperature: 65 °C and (L) 1 Kb GRS Ladder DNA (Grisp). The sequence length is expressed in bp.

As observed in Figure 19, all the PCR products have the expected sizes to be used in the yeast transformation. After transformation, it was possible to recover several transformants for each transformation (T1 and T2) after plating on selective media, while no colonies were observed for the negative control (transformation only with the linearized YAC).

To assess if the phage genomes were correctly assembled in the YAC, the yeast transformants were screened by yeast colony PCR using a set of primers placed upstream and downstream of the gene insertion sites (**Table 15**). The products of each yeast colony PCR were visualized on a 1 % (w/v) electrophoresis agarose gel, as shown in **Figure 20**.

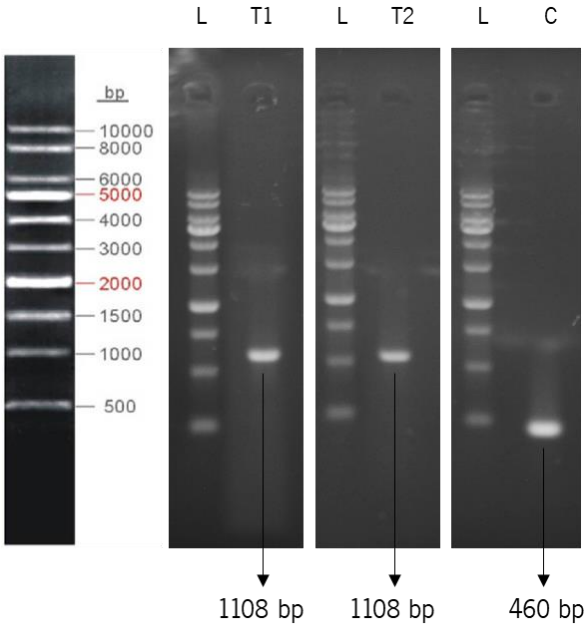

Figure 20 - Gel electrophoresis showing the amplification of one correct transformant for each yeast transformation. (C) control – original sequence, and (L) 1 Kb GRS Ladder DNA (Grisp). The DNA sizes presented include the size of the original sequence plus an additional 648 bp correspondent to the amplification of the *gp*55 from A2 phage.

Figure 20 shows bands with the expected sizes of amplification for each transformation (T1: 1108 bp; T2 1108 bp; Control: 460 bp), which confirms that gp55 from phage A2 was successfully cloned into PE3Δgp1–gp12 phage for T1 and PE3Δgp1–gp12:Nluc phage for T2. These positive yeast clones were then used for yeast DNA extraction in order to recover the YAC-phage DNA. After DNA extraction from yeast cells, 500 ng of the constructs (YAC-phage DNA) were transformed into the *P. aeruginosa* PAO1 host, which allows phage genes to be transcribed and produce functional phages in case the gene insertion does not alter the viability of the phage. In this step, the transformation was via electroporation due to the superior efficacy compared to the heat-shock approach (Yoshida & Sato, 2009).

In fact, phage plaques were observed after plating, but only for T2 even after three attempts. In order to recover plaques from T1, it would probably be essential to do some optimizations of the DNA concentration to be electroporated or incubation time after electroporation. Since phage plaques were obtained for T2, the work proceeded with this newly engineered phage as this was the phage already carrying the Nluc gene that can be used for detection. The resulting phage plaques obtained from electroporation were picked and the recombinant phage was produced and checked by PCR using the set of primers described above. The electrophoresis gel and the Sanger sequencing revealed that the

insertion of the TFP from phage A2 into the genome of phage PE3Δgp1–gp12 was successfully done (**Figure 21**).

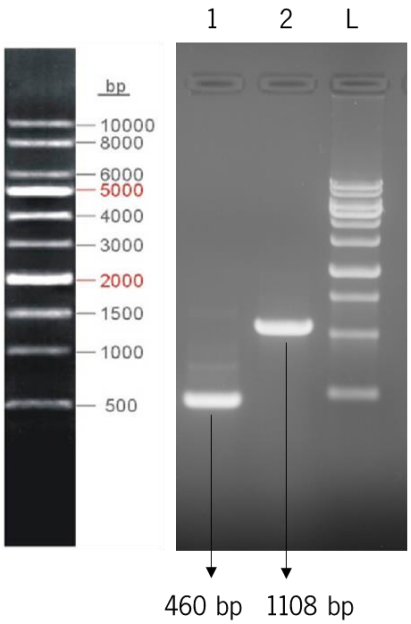

Figure 21 – Wild-type phage versus chimeric phage. (1) PE3 phage; (2) PCR-based confirmation of the insertion of A2*gp*55 in the genome of phage PE3Δgp1–gp12:Nluc and (L) 1 Kb GRS Ladder DNA (Grisp). The sequence length is expressed in bp.

After propagation of recombinant phage and confirmation of the correct assembly, a new analysis of the host range was performed to understand if the addition of a new TFP did actually result in the ability of the engineered phage to target a wider range of strains compared to wild-type phage. This would be a great advantage as currently, the most popular method for achieving a wider host range is the combination of multiple phages with various host ranges into a single cocktail, which is always a time-consuming process. The host range of the four phages A2, PE3 WT, PE3Δgp1–gp12:Nluc and T2 were tested against a panel of 52 *P. aeruginosa* clinical strains by spot test. **Table 18** shows the results of the lytic spectra.

Table 18 - EOP of the A2, PE3 WT, PE3Δgp1–gp12:Nluc and recombinant T2 phages against different strains of *P. aeruginosa*

Phage / Strain	A2	PE3	PE3Δgp1–gp12:Nluc	T2
1	0.5	-	-	LFW
2	-	-	-	-

3	<0.001	-	-	-
4	LFW	-	-	LFW
5	0.4	0.3	0.4	0.1
6	0.4	0.6	0.4	0.004
7	<0.001	-	-	-
8	LFW	LFW	LFW	LFW
9	LFW	-	-	LFW
10	-	-	-	-
11	-	0.3	LFW	LFW
12	LFW	0.3	LFW	LFW
14	-	-	-	-
15	LFW	-	-	-
16	0.1	0.3	0.4	LFW
17	-	0.1	LFW	LFW
18	0.005	-	-	LFW
19	-	-	-	-
20	0.006	LFW	-	LFW
21	0.4	0.3	0.004	0.005
22	0.1	-	-	LFW
23	LFW	0.3	0.8	<0.001
24	-	-	-	-
25	0.5	-	-	LFW
26	-	LFW	LFW	LFW
27	0.1	0.4	LFW	LFW
28	0.2	<0.001	LFW	LFW
29	0.1	LFW	LFW	LFW
A22	0.2	LFW	LFW	LFW
A63	-	-	-	-
A64	LFW	LFW	LFW	LFW

A65	LFW	0.2	0.4	LFW
A66	LFW	LFW	LFW	LFW
A67	LFW	LFW	LFW	LFW
A69	LFW	0.3	LFW	LFW
A70	0.8	-	-	LFW
A71	LFW	-	-	-
052EX	-	LFW	LFW	LFW
O64	LFW	-	-	LFW
O65	-	0.004	0.4	<0.001
O77	LFW	-	-	LFW
O78	0.2	0.2	LFW	LFW
O79	0.2	LFW	LFW	LFW
O92	-	0.1	0.020	<0.001
144	0.5	0.5	LFW	LFW
149	-	-	-	-
wzy	LFW	0.4	0.1	0.006
wbpL	-	0.1	0.007	LFW
rmlC	-	-	-	-
rmd	0.1	0.5	0.6	0.1
PAO1	1.0	1.0	1.0	1.0
PA14	-	-	-	LFW
% infection	54	51	31	23
% high productive infection	13	10	8	2

Contrary to what was expected, the recombinant phage, named T2, did not reveal a broader host range. Although it was expected that this phage would also be able to infect the *P. aeruginosa* strains that are infected by phage A2 leading to a 58 % infection rate, this was not observed and the engineered phage

revealed a narrower host range. In fact, T2 was only able to infect 12 strains, which is even less than the number infected by the PE3gp1-gp12:Nluc phage that was used as a scaffold.

So far, some studies have taken advantage of the fact that host range is connected to tail fiber composition for specific phages to show that the host ranges of phages can be changed or expanded. For instance, in order to particularly target *E. coli* O157:H7, Yoichi et al., (2005) genetically altered a T2 phage by replacing the long tail fiber genes with those from phage PP01. The exchange was carried out through homologous recombination. Although it had the same host range as phage PP01 and had the PP01 genes gp37 and gp38, the recombinant phage T2ppD1 was unable to infect its original host, *E. coli* K-12 (Yoichi et al., 2005). Lin et al., (2012) developed a hybrid T3 and T7 phage (T3/7) by replacing a portion of the T3 tail fiber gene (gp17) with that of the T7 phage. Compared to either of the T3 or T7 wild-type phages, the T3/7 recombinant phage had a wider host range and greater adsorption efficiency (Lin et al., 2012).

By modularly replacing the components of the phage tail and using the yeast-based platform, Ando et al., (2015) were able to redirect *E. coli* phage scaffolds to target pathogenic *Yersinia* and *Klebsiella* bacteria, and *Klebsiella* phage scaffolds to target *E. coli*.

Although the promising results reported in the literature, here it was not possible to increase the phage host range through the insertion of the TFP from A2 phage in the PE3Δgp1–gp12:Nluc phage genome. A possible explanation is that the phage may need the other TFPs to acquire the same spectrum as A2 phage. Additionally, Pires et al., (2021) discovered that the deletion of genes gp1 to gp12 from PE3 phage resulted in a slight reduction of the host range of the phage; hence, some of these genes may be involved in host recognition, takeover or beginning of replication, which may explain the increase of LFW. In this regard, it would be interesting to clone new TFPs without deleting genes from the phage genome as a future step. However, as this leads to an increase in the size of the phage genome, it can be a challenge due to the phage's capacity to encapsulate DNA. Although the phage genomic modification did not result in the expected outcome, it was possible to demonstrate that the yeast-based phage-engineering strategy is an efficient and robust method to engineer the genomes of *P. aeruginosa* phages and can be easily applied in the future to perform other modifications as mentioned above that may result in host range increase (Pires et al., 2021).

Chapter 4

CONCLUSIONS AND FUTURE PERSPECTIVES

4. CONCLUSIONS AND FUTURE PERSPECTIVES

4.1. Conclusions

Hospital infections are a public health problem worldwide. *Pseudomonas aeruginosa* is a major cause of nosocomial infections and its early detection is crucial for the effective treatment of these infections. In addition, its high resistance to a wide range of antibiotics has opened the door to the world of phage therapy. Phages have great potential against bacterial diseases, however they have a limited host range. Using phage engineering tools, it is possible to assemble chimeric phages with expanded host ranges and therefore capable of targeting a wider range of strains. These phages can also encode reporter genes, resulting in a fast and accurate tool for detecting bacteria in clinical settings, thus replacing conventional culture methods that are often time-consuming. The main objectives of this work were i) the development of a tool for rapid detection of *P. aeruginosa* and ii) the identification of TFP for cloning, expression, purification and functional analysis of these proteins for further genome engineering.

The reporter phage, PE3Δgp1–gp12:Nluc, is capable of detecting at least 620 CFU in 1 mL of sample contaminated with *P. aeruginosa* PAO1, in less than 8 h. Overall, the NanoLuc-based reporter phage allows for the rapid, specific and sensitive detection and differentiation of viable *P. aeruginosa* cells using a simple protocol, 41 h faster than culture-dependent approaches (Tramper-stranders et al., 2005). Despite the fact that not all clinical strains tested by this reporter phage were detected, it was found that in those cases where it was, the minimum detectable concentration was only 10 times higher than the detection of the host strain. Therefore, this phage-based detection system is a promising alternative to the common methods for the accurate detection of viable *P. aeruginosa* PAO1 in clinical settings, enabling diagnosis within a working day.

Two annotated potential TFPs from phage A2 and five potential TFPs from PE3 phage were successfully cloned and expressed by heterologous recombination. Their binding capacity was tested by epifluorescence microscopy and only pGFP_A2gp55 protein showed the ability to bind to host strains which indicates that it is a functional TFP.

The yeast-based phage-engineering strategy was used to successfully insert the functional TFP (*gp*55) from A2 phage on PE3Δgp1–gp12:Nluc phage genome. Still, this approach did not increase the phage host range. Although it was proved the binding ability of A2gp55 by functional analysis and by the ability of the modified phage to produce lysis from without, it seems that this A2 phage TFP does not allows a phage adsorption that triggers phage infection.

4.2. Future perspectives

The phage-based detection system was used in a limited number of strains and should be tested in a wider range of clinical strains. Furthermore, the methodology needs to be assessed in real samples such as blood, urine, or other fluids. Also, the phage used in this methodology has a limited host range, which is a problem that can lead to false negatives. This suggests that the phage can be modified to improve the number of target strains that it can infect and consequently its sensitivity.

More research is required to determine why the remaining proteins aren't functional TFPs since they don't bind to host strains. However, it is possible that the remaining proteins, that do not bind to host strain, require the presence of other phage proteins to acquire the functional structure. Another possibility is that the studied proteins under investigation are not truly TFPs and are not crucial for host recognition.

Additionally, the yeast-based phage-engineering strategy did not increase the phage host spectrum. It would be interesting to try to clone new TFPs in the future without eliminating genes from the phage. However, because the phage may encapsulate DNA, this results in an expansion of the phage genome, which might be problematic.

Chapter 5

REFERENCES

5. REFERENCES

Abedon, S. T. (2011). Lysis from without. *Bacteriophage*, *1*(1), 46–49. https://doi.org/10.4161/bact.1.1.13980

Agilent Technologies. (2015). ArcticExpress™ competent cells. *Arctic Express Instruction Manual*. www.genomics.agilent.com

Anbu, P., Gopinath, S. C. B., Chaulagain, B. P., & Lakshmipriya, T. (2017). Microbial Enzymes and Their Applications in Industries and Medicine 2016. *BioMed Research International*, *2017*. https://doi.org/10.1155/2017/2195808

Ando, H., Lemire, S., Pires, D. P., & Lu, T. K. (2015). Engineering Modular Viral Scaffolds for Targeted Bacterial Population Editing. *Cell Systems*, *1*(3), 187–196. https://doi.org/10.1016/j.cels.2015.08.013

Bassetti, M., Vena, A., Croxatto, A., Righi, E., & Guery, B. (2018). How to manage Pseudomonas aeruginosa infections. *Drugs in Context*, *7*(212527), 1–18. https://doi.org/10.7573/dic.212527

Breidenstein, E. B. M., de la Fuente-Núñez, C., & Hancock, R. E. W. (2011). Pseudomonas aeruginosa: All roads lead to resistance. *Trends in Microbiology*, *19*(8), 419–426. https://doi.org/10.1016/j.tim.2011.04.005

Burns, J. L., Gibson, R. L., Mcnamara, S., Yim, D., Emerson, J., Rosenfeld, M., Hiatt, P., Mccoy, K., Castile, R., Smith, A. L., & Ramsey, B. W. (2001). Longitudinal Assessment of Pseudomonas aeruginosa in Young Children with Cystic Fibrosis. *The Journal of Infectious Diseases*, *183*(3), 444–452. https://doi.org/10.1086/318075

Centers for Disease Control and Prevention. (2019). *Multidrug-Resistant Pseudomonas aeruginosa*. https://www.cdc.gov/drugresistance/pdf/threats-report/pseudomonas-aeruginosa-508.pdf

Chatterjee, M., Anju, C. P., Biswas, L., Anil Kumar, V., Gopi Mohan, C., & Biswas, R. (2016). Antibiotic resistance in Pseudomonas aeruginosa and alternative therapeutic options. *International Journal of Medical Microbiology*, *306*(1), 48–58. https://doi.org/10.1016/j.ijmm.2015.11.004

Choi, K. H., Kumar, A., & Schweizer, H. P. (2006). A 10-min method for preparation of highly electrocompetent Pseudomonas aeruginosa cells: Application for DNA fragment transfer between chromosomes and plasmid transformation. *Journal of Microbiological Methods*, *64*(3), 391–397. https://doi.org/10.1016/j.mimet.2005.06.001

Ciofu, O., & Tolker-nielsen, T. (2019). Tolerance and Resistance of Pseudomonas aeruginosa Biofilms to

Antimicrobial Agents — How P . aeruginosa Can Escape Antibiotics. *Frontiers in Microbiology*, *10*(913), 15. https://doi.org/10.3389/fmicb.2019.00913

Costa, S. P., Dias, N. M., Melo, L. D. R., Azeredo, J., Santos, S. B., & Carvalho, C. M. (2020). A novel flow cytometry assay based on bacteriophage-derived proteins for Staphylococcus detection in blood. *Nature*, *10*, 1–13. https://doi.org/10.1038/s41598-020-62533-7

Costa, S. P., Nogueira, C. L., Cunha, A. P., Lisac, A., Costa, S. P., Nogueira, C. L., Cunha, A. P., & Lisac, A. (2022). Potential of bacteriophage proteins as recognition molecules for pathogen detection. *Critical Reviews in Biotechnology*, 1–18. https://doi.org/10.1080/07388551.2022.2071671

Davies, E. V, Winstanley, C., Fothergill, J. L., & James, C. E. (2016). The role of temperate bacteriophages in bacterial infection. *FEMS Microbiology Letters*, *363*(5), 1–10. https://doi.org/10.1093/femsle/fnw015

de Kievit, T. R., Dasgupta, T., Schweizer, H., & Lam, J. S. (1995). Molecular cloning and characterization of the rfc gene of Pseudomonas aeruginosa (serotype O5). *Molecular Microbiology*, *16*(3), 565–574. https://doi.org/10.1111/j.1365-2958.1995.tb02419.x

Dixon, A. S., Schwinn, M. K., Hall, M. P., Zimmerman, K., Otto, P., Lubben, T. H., Butler, B. L., Binkowski, B. F., MacHleidt, T., Kirkland, T. A., Wood, M. G., Eggers, C. T., Encell, L. P., & Wood, K. V. (2016). NanoLuc Complementation Reporter Optimized for Accurate Measurement of Protein Interactions in Cells. *ACS Chemical Biology*, *11*(2), 400–408. https://doi.org/10.1021/acschembio.5b00753

Domingo-Calap, P., & Delgado-Martínez, J. (2018). Bacteriophages : Protagonists of a Post-Antibiotic Era. *Antibiotics*, *7*(66), 1–16. https://doi.org/10.3390/antibiotics7030066

Drulis-kawa, Z., Majkowska-skrobek, G., Maciejewska, B., Delattre, A., & Lavigne, R. (2012). Learning from Bacteriophages - Advantages and Limitations of Phage and Phage-Encoded Protein Applications. *Current Protein and Peptide Science*, *13*(8), 699–722. https://doi.org/10.2174/138920312804871193

Erickson, S., Paulson, J., Brown, M., Hahn, W., Gil, J., Barron-Montenegro, R., Moreno-Switt, A. I., Eisenberg, M., & Nguyen, M. M. (2021). Isolation and engineering of a Listeria grayi bacteriophage. *Scientific Reports*, *11*(1), 1–12. https://doi.org/10.1038/s41598-021-98134-1

Ghysels, B., Fajardo, A., & Martı, N. (2008). The Neglected Intrinsic Resistome of Bacterial Pathogens. *PLoS ONE*, *3*(2), 1–6. https://doi.org/10.1371/journal.pone.0001619

Hagens, S., Habel, A., Ahsen, U. Von, Gabain, A. Von, & Blasi, U. (2004). Therapy of Experimental Pseudomonas Infections with a Nonreplicating Genetically Modified Phage. *Antimicrobial Agents and*

Chemotherapy, *48*(10), 3817–3822. https://doi.org/10.1128/AAC.48.10.3817

Heinz, E., Ejaz, H., Scott, J. B., Wang, N., Guanjaran, S., Pickard, D., Wilksch, J., Cao, H., Ikram-ul-Haq, Dougan, G., & Strugnell, R. A. (2019). Resistance mechanisms and population structure of highly drug resistant Klebsiella in Pakistan during the introduction of the carbapenemase NDM-1. *Scientific Reports*, *9*(2392), 1–13. https://doi.org/10.1038/s41598-019-38943-7

Hinkley, T. C., Garing, S., Singh, S., Le Ny, A. L. M., Nichols, K. P., Peters, J. E., Talbert, J. N., & Nugen, S. R. (2018). Reporter bacteriophage T7NLC utilizes a novel NanoLuc::CBM fusion for the ultrasensitive detection of: Escherichia coli in water. *Analyst*, *143*(17), 4074–4082. https://doi.org/10.1039/c8an00781k

Hogardt, M., Trebesius, K., Geiger, A. M., Hornef, M., Heesemann, R., & Pettenkofer-institut, M. Von. (2000). Specific and Rapid Detection by Fluorescent In Situ Hybridization of Bacteria in Clinical Samples Obtained from Cystic Fibrosis Patients. *Journal of Clinical Microbiology*, *38*(2), 818–825. https://doi.org/10.1128/jcm.38.2.818-825.2000

Jones, H. J., Shield, C. G., & Swift, B. M. C. (2020). The Application of Bacteriophage Diagnostics for Bacterial Pathogens in the Agricultural Supply Chain: From Farm-To-Fork. *PHAGE: Therapy, Applications, and Research*, *1*(4), 176–188. https://doi.org/10.1089/phage.2020.0042

Juan, C., Peña, C., & Oliver, A. (2017). Host and pathogen biomarkers for severe Pseudomonas aeruginosa infections. *Journal of Infectious Diseases*, *215*(Suppl 1), S44–S51. https://doi.org/10.1093/infdis/jiw299

Kakasis, A., & Panitsa, G. (2019). Bacteriophage therapy as an alternative treatment for human infections . A comprehensive review. *International Journal of Antimicrobial Agents*, *53*, 16–21. https://doi.org/10.1016/j.ijantimicag.2018.09.004

Klockgether, J., Cramer, N., Wiehlmann, L., Davenport, C. F., & Tümmler, B. (2011). Pseudomonas aeruginosa genomic structure and diversity. *Frontiers in Microbiology*, *2*(150), 1–18. https://doi.org/10.3389/fmicb.2011.00150

Kortright, K. E., Chan, B. K., Koff, J. L., & Turner, P. E. (2019). Review Phage Therapy : A Renewed Approach to Combat Antibiotic-Resistant Bacteria. *Cell Host and Microbe*, *25*(2), 219–232. https://doi.org/10.1016/j.chom.2019.01.014

Koskella, B., & Meaden, S. (2013). Understanding Bacteriophage Specificity in Natural Microbial Communities. *Viruses*, *5*(3), 806–823. https://doi.org/10.3390/v5030806

Lin, D. M., Koskella, B., Lin, H. C., Lin, D. M., Lin, H. C., & Gastroenterology, S. (2017). Phage therapy:

An alternative to antibiotics in the age of multi-drug resistance. *World Journal of Gastrointestinal Pharmacology and Therapeutics*, *8*(3), 162–173. https://doi.org/10.4292/wjgpt.v8.i3.162

Lin, T. Y., Lo, Y. H., Tseng, P. W., Chang, S. F., Lin, Y. T., & Chen, T. S. (2012). A T3 and T7 recombinant phage acquires efficient adsorption and a broader host range. *PLoS ONE*, *7*(2), 1–10. https://doi.org/10.1371/journal.pone.0030954

Loc-carrillo, C., & Abedon, S. T. (2011). Pros and cons of phage therapy. *Bacteriophage*, *1*(2), 111–114. https://doi.org/10.4161/bact.1.2.14590

Lu, T. K., & Collins, J. J. (2007). Dispersing biofilms with engineered enzymatic bacteriophage. *PNAS*, *104*(27), 11197–11202. https://doi.org/10.1073/pnas.0704624104

Lu, T. K., & Collins, J. J. (2009). Engineered bacteriophage targeting gene networks as adjuvants for antibiotic therapy. *PNAS*, *106*(12), 4629–4634. https://doi.org/10.1073/pnas.0800442106

Lucigen Corporation. (2018). *OverExpress ™ Chemically Competent cells*.

Matsuda, T., Freeman, T. A., Hilbert, D. W., Duff, M., Fuortes, M., Stapleton, P. P., & Daly, J. M. (2005). Lysis-deficient bacteriophage therapy decreases endotoxin and inflammatory mediator release and improves survival in a murine peritonitis model. *Surgery*, *137*(6), 639–646. https://doi.org/10.1016/j.surg.2005.02.012

Meile, S., Kilcher, S., Loessner, M. J., & Dunne, M. (2020). Reporter Phage-Based Detection of Bacterial Pathogens : Design Guidelines and Recent Developments. *Viruses*, *12*(944), 25. https://doi.org/doi:10.3390/v12090944

Meile, S., Sarbach, A., Du, J., Schuppler, M., Saez, C., Loessner, M. J., & Kilcher, S. (2020). Engineered reporter phages for rapid bioluminescence-based detection and differentiation of viable Listeria cells. *Applied and Environmental Microbiology*, *86*(11), 1–14. https://doi.org/10.1128/AEM.00442-20

Mirzaei, M. K., & Nilsson, A. S. (2015). Isolation of phages for phage therapy: A comparison of spot tests and efficiency of plating analyses for determination of host range and efficacy. *PLoS ONE*, *10*(3), 1–13. https://doi.org/10.1371/journal.pone.0118557

Monteiro, R., Pires, D. P., Costa, A. R., & Azeredo, J. (2019). Phage Therapy : Going Temperate ? *Trends in Microbiology*, *27*(4), 368–378. https://doi.org/10.1016/j.tim.2018.10.008

Moradali, M. F., Ghods, S., & Rehm, B. H. A. (2017). Pseudomonas aeruginosa Lifestyle : A Paradigm for Adaptation , Survival , and Persistence. *Frontiers in Cellular and Infection Microbiology*, *7*(39), 29. https://doi.org/10.3389/fcimb.2017.00039

Motlagh, A. M., Bhattacharjee, A. S., & Goel, R. (2016). Biofilm control with natural and genetically-

modified phages. *World Journal of Microbiology and Biotechnology*, *32*(67), 10. https://doi.org/10.1007/s11274-016-2009-4

Nair, A., & Khairnar, K. (2019). Genetically engineered phages for therapeutics : proceed with caution. *Nature Medicine*, *25*(1028), 1. https://doi.org/10.1038/s41591-019-0506-3

Nguyen, L., Garcia, J., Gruenberg, K., & MacDougall, C. (2018). Multidrug-Resistant Pseudomonas Infections: Hard to Treat, But Hope on the Horizon? *Current Infectious Disease Reports*, *20*(8), 10. https://doi.org/10.1007/s11908-018-0629-6

Nguyen, M. M., Gil, J., Brown, M., Cesar Tondo, E., Soraya Martins de Aquino, N., Eisenberg, M., & Erickson, S. (2020). Accurate and sensitive detection of Salmonella in foods by engineered bacteriophages. *Scientific Reports*, *10*(1), 1–13. https://doi.org/10.1038/s41598-020-74587-8

North, O. I., Sakai, K., Yamashita, E., Nakagawa, A., Iwazaki, T., Büttner, C. R., Takeda, S., & Davidson, A. R. (2019). Phage tail fibre assembly proteins employ a modular structure to drive the correct folding of diverse fibres. *Nature Microbiology*, *4*(10), 1645–1653. https://doi.org/10.1038/s41564-019-0477-7

Pachori, P., Gothalwal, R., & Gandhi, P. (2019). Emergence of antibiotic resistance Pseudomonas aeruginosa in intensive care unit ; a critical review. *Genes & Diseases*, *6*(2), 109–119. https://doi.org/10.1016/j.gendis.2019.04.001

Pang, Z., Raudonis, R., Glick, B. R., Lin, T. J., & Cheng, Z. (2019). Antibiotic resistance in Pseudomonas aeruginosa: mechanisms and alternative therapeutic strategies. *Biotechnology Advances*, *37*(1), 177–192. https://doi.org/10.1016/j.biotechadv.2018.11.013

Passador, L., Cook, J. M., Gambello, M. J., Rust, L., & Iglewski, B. H. (1993). Expression of Pseudomonas aeruginosa virulence genes requires cell-to-cell communication. *Science*, *260*(5111), 1127–1130. https://doi.org/10.1126/science.8493556

Pereira, S. G., Rosa, A. C., Ferreira, A. S., Moreira, L. M., Proença, D. N., Morais, P. V., & Cardoso, O. (2014). Virulence factors and infection ability of Pseudomonas aeruginosa isolates from a hydropathic facility and respiratory infections. *Journal of Applied Microbiology*, *116*(5), 1359–1368. https://doi.org/10.1111/jam.12463

Pires, D., Melo, L., Vilas Boas, D., Sillankorva, S., & Azeredo, J. (2017). Phage therapy as an alternative or complementary strategy to prevent and control biofilm-related infections. *Current Opinion in Microbiology*, *39*, 48–56. https://doi.org/10.1016/j.mib.2017.09.004

Pires, D. P., Cleto, S., Sillankorva, S., Azeredo, J., & Lu, T. K. (2016). Genetically Engineered Phages: a

Review of Advances over the Last Decade. *Microbiology and Molecular Biology Reviews*, *80*(3), 523–543. https://doi.org/10.1128/mmbr.00069-15

Pires, D. P., Costa, A. R., Meneses, L., & Azeredo, J. (2020). Current challenges and future opportunities of phage therapy. *FEMS Microbiology Letters*, *44*(6), 684–700. https://doi.org/10.1093/femsre/fuaa017

Pires, D. P., Dötsch, A., Anderson, E. M., Hao, Y., Khursigara, C. M., Lam, J. S., Sillankorva, S., & Azeredo, J. (2017). A genotypic analysis of five P. aeruginosa strains after biofilm infection by phages targeting different cell surface receptors. *Frontiers in Microbiology*, *8*(1229), 1–14. https://doi.org/10.3389/fmicb.2017.01229

Pires, D. P., Kropinski, A. M., Azeredo, J., & Sillankorva, S. (2014). Complete genome sequence of the Pseudomonas aeruginosa bacteriophage phiIBB-PAA2. *Genome Announcements*, *2*(1), 7–8. https://doi.org/10.1128/genomeA.e01102-13

Pires, D. P., Monteiro, R., Mil-Homens, D., Fialho, A., Lu, T. K., & Azeredo, J. (2021). Designing P. aeruginosa synthetic phages with reduced genomes. *Scientific Reports*, *11*(1), 1–10. https://doi.org/10.1038/s41598-021-81580-2

Pirnay, J.-P., Vos, D. De, Verbeken, G., Merabishvili, M., Chanishvili, N., Vaneechoutte, M., Zizi, M., Laire, G., Lavigne, R., Huys, I., Mooter, G. Van den, Buckling, A., Debarbieux, L., Pouillot, F., Azeredo, J., Kutter, E., Dublanchet, A., Górski, A., & Adamia, R. (2011). The Phage Therapy Paradigm: Prêt-à-Porter or Sur-mesure ? *Pharm Res*, *28*, 934–937. https://doi.org/10.1007/s11095-010-0313-5

Pirnay, J., Verbeken, G., Ceyssens, P., Huys, I., Vos, D. De, Ameloot, C., & Fauconnier, A. (2018). The Magistral Phage. *Viruses*, *10*(2), 1–7. https://doi.org/10.3390/v10020064

Principi, N., Silvestri, E., & Esposito, S. (2019). Advantages and Limitations of Bacteriophages for the Treatment of Bacterial Infections. *Frontiers in Pharmacology*, *10*(513), 1–9. https://doi.org/10.3389/fphar.2019.00513

Rahim, R., Burrows, L. L., Monteiro, M. A., Perry, M. B., & Lam, J. S. (2000). Involvement of the rml locus in core oligosaccharide and O polysaccharide assembly in Pseudomonas aeruginosa. *Microbiology*, *146*(11), 2803–2814. https://doi.org/10.1099/00221287-146-11-2803

Reuter, K., Steinbach, A., & Helms, V. (2016). Interfering with Bacterial Quorum Sensing. *Perspectives in Medical Chemistry*, *8*, 1–15. https://doi.org/10.4137/PMC.S13209

Ribeiro, H. G., Melo, L. D. R., Oliveira, H., Boon, M., Lavigne, R., Noben, J.-P., Azeredo, J., & Oliveira, A. (2019). Characterization of a new podovirus infecting Paenibacillus larvae. *Scientific Reports*,

9(20355), 1–12. https://doi.org/10.1038/s41598-019-56699-y

Rocchetta, H. L., Burrows, L. L., Pacan, J. C., & Lam, J. S. (1998). Three rhamnosyltransferases responsible for assembly of the A-band D-rhamnan polysaccharide in Pseudomonas aeruginosa: A fourth transferase, WbpL, is required for the initiation of both A-band and B-band lipopolysaccharide synthesis (Molecular Mi. *Molecular Microbiology*, *28*(6), 1103–1119. https://doi.org/10.1046/j.1365-2958.1998.01109.x

Rocchetta, H. L., Pacan, J. C., & Lam, J. S. (1998). Synthesis of the A-band polysaccharide sugar D-rhamnose requires Rmd and WbpW: Identification of multiple AlgA homologues, WbpW and ORF488, in Pseudomonas aeruginosa. *Molecular Microbiology*, *29*(6), 1419–1434. https://doi.org/10.1046/j.1365-2958.1999.0erat.x

Rohde, C., Wittmann, J., & Kutter, E. (2018). Bacteriophages: A therapy concept against multi-drug-resistant bacteria. *Surgical Infections*, *19*(8), 737–744. https://doi.org/10.1089/sur.2018.184

Santos, S. B., Cunha, A. P., Macedo, M., Nogueira, C. L., Brandão, A., Costa, S. P., Melo, L. D. R., Azeredo, J., & Carvalho, C. M. (2020). Bacteriophage - receptor binding proteins for multiplex detection of Staphylococcus and Enterococcus in blood. *Biotechnology Advances*, *117*, 3286–3298. https://doi.org/10.1002/bit.27489

Schmelcher, M., & Loessner, M. J. (2008). *Principles of Bacterial Detection : Biosensors, Recognition Receptores and Microsystems*.

Schmelcher, M., & Loessner, M. J. (2014). Application of bacteriophages for detection of foodborne pathogens. *Bacteriophage*, *4*(e28137), 1–14. https://doi.org/10.4161/bact.28137

Silby, M. W., Winstanley, C., Godfrey, S. A. C., Levy, S. B., & Jackson, R. W. (2011). Pseudomonas genomes: Diverse and adaptable. *FEMS Microbiology Reviews*, *35*(4), 652–680. https://doi.org/10.1111/j.1574-6976.2011.00269.x

Strateva, T., & Mitov, I. (2011). Contribution of an arsenal of virulence factors to pathogenesis of Pseudomonas aeruginosa infections. *Annals of Microbiology*, *61*(4), 717–732. https://doi.org/10.1007/s13213-011-0273-y

Tagliaferri, T. L., Jansen, M., & Horz, H.-P. (2019). Fighting Pathogenic Bacteria on Two Fronts: Phages and Antibiotics as Combined Strategy. *Frontiers in Cellular and Infection Microbiology*, *9*(22), 13. https://doi.org/10.3389/fcimb.2019.00022

Takahashi, Y., & Tatsuma, T. (2014). Metal oxides and hydroxides as rechargeable materials for photocatalysts with oxidative energy storage abilities. *Electrochemistry*, *82*(9), 749–751.

https://doi.org/10.5796/electrochemistry.82.749

Tang, Y., Ali, Z., Zou, J., Jin, G., Zhu, J., Yang, J., & Dai, J. (2017). Detection methods for: Pseudomonas aeruginosa: History and future perspective. *RSC Advances*, *7*(82), 51789–51800. https://doi.org/10.1039/c7ra09064a

Torres-Barceló, C. (2018). Phage Therapy Faces Evolutionary Challenges. *Viruses*, *10*(323), 8. https://doi.org/10.3390/v10060323

Tramper-stranders, G. A., Ent, C. K. Van Der, & Wolfs, T. F. W. (2005). Detection of Pseudomonas aeruginosa in patients with cystic fibrosis. *Journal of Cystic Fibrosis*, *4*(2), 37–43. https://doi.org/10.1016/j.jcf.2005.05.009

Viazis, S., Akhtar, M., Feirtag, J., Brabban, A. D., & Diez-Gonzalez, F. (2011). Isolation and characterization of lytic bacteriophages against enterohaemorrhagic Escherichia coli. *Journal of Applied Microbiology*, *110*(5), 1323–1331. https://doi.org/10.1111/j.1365-2672.2011.04989.x

Waters, E. M., Neill, D. R., Kaman, B., Sahota, J. S., Clokie, M. R. J., Winstanley, C., & Kadioglu, A. (2017). Phage therapy is highly effective against chronic lung infections with Pseudomonas aeruginosa. *Thorax*, *0*(0), 2. https://doi.org/10.1136/thoraxjnl-2016-209265

World Health Organization. (2017). *WHO publishes list of bacteria for which new antibiotics are urgently needed*. https://www.who.int/news/item/27-02-2017-who-publishes-list-of-bacteria-for-which-new-antibiotics-are-urgently-needed

Xu, J., Moore, J. E., Murphy, P. G., Millar, B. C., & Elborn, S. (2004). Early detection of Pseudomonas aeruginosa – comparison of conventional versus molecular (PCR) detection directly from adult patients with cystic fibrosis (CF). *Annals of Clinical Microbiology and Antimicrobials*, *3*(21), 1–5. https://doi.org/10.1186/1476-0711-3-21

Yoichi, M., Abe, M., Miyanaga, K., Unno, H., & Tanji, Y. (2005). Alteration of tail fiber protein gp38 enables T2 phage to infect Escherichia coli O157:H7. *Journal of Biotechnology*, *115*(1), 101–107. https://doi.org/10.1016/j.jbiotec.2004.08.003

Yoshida, N., & Sato, M. (2009). Plasmid uptake by bacteria : a comparison of methods and efficiencies. *Applied Microbiology and Biotechnology*, *83*(5), 791–798. https://doi.org/10.1007/s00253-009-2042-4

Young, J. S., Gormley, E., & Wellington, E. M. H. (2005). Molecular detection of Mycobacterium bovis and Mycobacterium bovis BCG (Pasteur) in soil. *Applied and Environmental Microbiology*, *71*(4), 1946–1952. https://doi.org/10.1128/AEM.71.4.1946-1952.2005

Supplementary material

Strains, bacteriophages and plasmids used in this work can be seen in the **Table S1**.

Table S1 - Bacterial strains, bacteriophages and plasmids used in this study

Strain, bacteriophage, or plasmid	Reference or source
P. aeruginosa strains	
PAO1	German Collection of Microorganisms and Cell Cultures (DSM22644)
PA14	Laboratory stock
1	Urine
2	Skin
3	Ear
4	Bronchial
5	Hemoculture
6	Urine
7	Ear
8	Urine
9	Urine
10	Urine
11	Skin ulcer
12	Expectoration
14	Urine
15	Skin ulcer
16	Skin ulcer
17	Catheter
18	Ear
19	Skin ulcer
20	Urine
21	Urine
22	Hemoculture
23	Urine

24	Expectoration
25	Expectoration
26	Ear
27	Unknown
28	Unknown
29	Unknown
A22	Unknown
A63	Expectoration
A64	Bronchial
A65	Bronchial
A66	Bronchial
A67	Bronchial
A69	Bronchial
A70	Bronchial
A71	Expectoration
052EX	Expectoration
O64	Hemoculture
O65	Bronchial
O77	Unknown
O78	Unknown
O79	Unknown
O92	Unknown
144	Unknown
149	Unknown
wzy	(A+B−), deficient in O-antigen polymerase for B-band biosynthesis, produces core-plus-one O-repeat unit (de Kievit et al., 1995)
wbpL	(A−B−), deficient in the initial glycosyltransferase affecting both B-band

	and A-band (Rocchetta, Burrows, et al., 1998)
rmlC	(A−B−), defective in TDP-L-rhamnose biosynthesis, with truncated outer core (Rahim et al., 2000)
rmd	(A−B+), deficient in GDP-D-rhamnose biosynthesis becomes A-band minus, not affecting B-band (Rocchetta, Pacan, et al., 1998)
E. coli strains	
Arctic express	Laboratory stock
C43	Laboratory stock
BL21	Laboratory stock
A51	Bronchial
Saccharomyces cerevisiae strains	
BY4741	Laboratory stock
Klebsiella pneumoniae strains	
A36	Bronchial
A57	Bronchial
Staphylococcus aureus strains	
A1	Bronchial - MRSA (Multi-Resistent *S. aureus*)
A9	Hemoculture - MRSA (Multi-Resistent *S. aureus*)
A39	Bronchial - MSSA (Multi-Sensitive *S. aureus*)
Enterococcus faecalis strains	
A74	Urine
Enterococcus faecium strains	
A78	Skin ulcer
Bacteriophages	
PE1	-

phiIBB-PAA2	Accession number: NC_022971.1
vB_PaeM_CEB_DP1	Accession number: KR869157
PA14G	-
PA14-20	-
vB_PaeP_PE3	Accession number: MN901924.1
PE3Δgp1–gp12	D. P. Pires et al., (2021)
PE3Δgp1–gp12:Nluc	This work
Plasmids	
pRS415	ATCC 87520
pGFP	Laboratory stock

Nucleotide and amino acid sequence of genes 53 and 55 belonging to phage A2 and genes 39, 44, 45, 46 and 47 belonging to phage PE3 are shown in the following table (**Table S2**).

Table S2 - Sequence of nucleotides and amino acids of the genes used at this work

Phage	Gene	Sequence	Annotated translation
A2	53	ATGGCCTCCCTTCCTCAGAAGCTGTTCGCTATAGGACAGAATATAGGTGGTGGGC AGGAGCGGGTACAGTTGAGCCGTCAAGGTTCCTACCGCCCCACCCACCTTGGGA CAATGCAATCGGGAGAGTCTAGTGGACAATCAAACCCTTTTGGCGCAATGGGCGG AGCAGCACTCGCGGCTCTCCTCGGGCAAGGAAGTGAGCCTTCTTCAGAAACAGTA CCAAGCTTTTCTGTCGAGGGGGCTAGAGGAGCAAGCGAACGAGGCGCAGCGGAA GTTGCAGCAGGTATGGGAGCGGGAGTGGGAATCCTTCCTAGCGCAGAAGAACTCG GTTTCGGACAGCAGCCAAAGTCTGGAATCCTAAGTAAACTATTTGGAGGTTAA	MASLPQKLFAIGQNIGGGQERVQLSRQGSYRPTHLGTMQS GESSGQSNPFGAMGGAALAALLGQGSEPSSETVPSFSVEG ARGASERGAAEVAAGMGAGVGILPSAEELGFGQQPKSGILS KLFGG
	55	ATGATTCATTTGATTACTCGTGAGAATATCGATCTGCTTCCTACCGTAGTCCCTGCT CTGGCCCGAGCCTTCAACAGGACGGACCTCGGTAAGTTTTGGGACTTCGAACACT TGGTTCACTCCTTGGTTAACTACGAGGCCTATGTCTTCTACCAAGAAGAGAGTGGC TACGCTGGTGTAATTCAAGTGTCCCAAGCACCCCTGGGTAACATCCTTCACTTCTT CTGGAGTGGTAAGATGCCTGGGAATGAAACCCCGGTAGATTACTCGGAGGTAGAC GACTTCCTCGGACAGTTCGCCCAACGAGTTAACTGTCGGTTTATCCAATGCGAAGG TCGTCGGGGCTGGAAGCCTACCCTAGAGAAACTCGGGTACACCGAAGACTCCGTA TCCTTCTATCGTGAGGTAACTCCAGATGAACTTCCTCCAATTTAA	MIHLITRENIDLLPTVVPALARAFNRTDLGKFWDFEHLVHS LVNYEAYVFYQEESGYAGVIQVSQAPLGNILHFFWSGKMPG NETPVDYSEVDDFLGQFAQRVNCRFIQCEGRRGWKPTLEK LGYTEDSVSFYREVTPDELPPI
PE3	39	ATGCTACTACTCGACGCAGTGAATGTCATCCTGCGCAAGATCGGCGAGCTGCCGA TCCCGAGCATGGATGAGACGTATCCAACCATGGCCATCGCCCTCCCGGAGCTGGA AGATCAACGCATCCAGTTGCTGACACAAGGCTGGTGGTTCAACACCTGGTGGAGG CACAAGCTGACACCTGACCCCACGGGCCGCATCAACCTGCCCAAGGGCACCTTG GCATTCTATCCGGATTCCCCGGACCTCCAGTGGGACGGCCTGGGGGTGCGAGAT GCCAACACCGGTGACGACCGCATCGGTAAGCCGGTCGAGGGCCGATTGGTGCTG TCTCGGGAGTGGGACCATATCCCGGAGATCGCACAGCGCGTCATTGCGCACCAG GCTGCGCTCGCGGTATACACTCACGAGATTGGACCGGACGAGACCGCCCAGGTC	MLLLDAVNVILRKIGELPIPSMDETYPTMAIALPELEDQRIQ LLTQGWWFNTWWRHKLTPDPTGRINLPKGTLAFYPDSPD LQWDGLGVRDANTGDDRIGKPVEGRLVLSREWDHIPEIAQ RVIAHQAALAVYTHEIGPDETAQVIAQELQAYQNELSRMHT RSRPLNTQAKRSFSRWRRSLRT

		ATCGCCCAGGAATTGCAGGCGTATCAGAACGAACTGTCCCGCATGCACACCCGAT CCCGTCCGCTGAACACCCAGGCCAAGCGTAGCTTCAGCCGGTGGCGGCGCAGCT TGAGGACCTGA	
PE3	44	GTGGCTCGGTTCAAGAATCCCGAGACCATCCACGTTGCAGATGGGGTCGAGGCTG TCTTCAGTCTCGACTTCCCGTTCCTGCGGCGTGAGGACGTATTCGTCCAGGTCGA TAAGATACTCGTCACCGACTATACGTGGGTAGACGACACCAACATCCAATTGGCC GTGGTGCCGAAGAAGGACCAAGAGGTCCGCATCTTCCGCGACACGCCCGCCCAG GTCCCGGACACACAGTTCAGCCAGGGCATCCCGTTCCTGCCTCGATACATCGACG CGAACAACAAGCAGCTCCTGTACGCTGTGCAGGAAGGCATCAACACCGCGAACCT CGCTCTCGATGGCGTACTCGACGCGATCCGTATCGCCGAGGAGGCTCGTCGCCT GGCGCAGGAAGCACTCGACGCCGCCAATGAGGCGCTTCGCCGTGCCCTGGGCTT CGCTGAGATTCGCACCGTGACCGAGGACTCGGATATTGATCCGAGCTGGCGGGGT TACTGGAACCGCTGCATCACTGCCGACAAGCCTCTGACCTTGACCATGCAGATGG AAGACCCGGATGCACCGTGGGTCGAGTTCAGCGAGGTTCACTTCGAGCAGGCCG GTGTGCGTGATCTAAACATCGTAGCCGGTCCTGGCGTTACCATCAACCGTTTGCA GAACACCACCATGCAGCTCTACGGCGAGAATGGCGTGTGTACTCTCAAGCGGCTG GGCGCTAACCACTGGATCGTGTTCGGGGCCATGGAGGACGAATAA	MARFKNPETIHVADGVEAVFSLDFPFLRREDVFVQVDKILV TDYTWVDDTNIQLAVVPKKDQEVRIFRDTPAQVPDTQFSQ GIPFLPRYIDANNKQLLYAVQEGINTANLALDGVLDAIRIAEE ARRLAQEALDAANEALRRALGFAEIRTVTEDSDIDPSWRGY WNRCITADKPLTLTMQMEDPDAPWVEFSEVHFEQAGVRD LNIVAGPGVTINRLQNTTMQLYGENGVCTLKRLGANHWIVF GAMEDE
	45	ATGCGCGGCATTATCGCGGGCATCATGGCCTCCCAAATTCGACGGCCCAAGCCCA TCCTGGCGACCTACCCGTATCCCATCATGGAGGCGGATAATCGCTGGGCTGCTCG GCCCAATATCGTGGCAGCTCTGACCAGGGACACTCTGAAGGAAGTCCGGCCAGAA GACACGCTGGAGCACTACAGTGCAGCCACCGCTGTACTGGCCGCCAGCATGCGC AGCCTGACACAAACGGGCTACGGCGGGGCCTGGCCGTACCAGCTCGTAACAGGT GTGGCAGATACCACCCTCCGGTCGCTGGTGAAGTCTACTACGGTCGAGGCTCAGC CCTACCTAGCCACGCCGGCAATCCACTCGGCGGACCTGCGGGTAGTGCTCATTAT CTCGGATTACGAGGTAGAGCCGTTCCATTACACCCTGACCAACAGCCTTGTACAG GCGGAGCTGAAAAATGTTTAA	MRGIIAGIMASQIRRPKPILATYPYPIMEADNRWAARPNIVA ALTRDTLKEVRPEDTLEHYSAATAVLAASMRSLTQTGYGGA WPYQLVTGVADTTLRSLVKSTTVEAQPYLATPAIHSADLRVV LIISDYEVEPFHYTLTNSLVQAELKNV
	46	ATGTTTAAGACCGAAGTAAAGGGACGTTACACCCTGATTCGCCGCAAGGCGGACG GCACTCCGGTGGAGACTCTGGAGTTCGACAACATCATTACGAATGCGGGCCTGGA TTGGATCGCCGCTATGGATACCGACCTCATGGGCGAACCCGTAGCGGTCAGCACT	MFKTEVKGRYTLIRRKADGTPVETLEFDNIITNAGLDWIAA MDTDLMGEPVAVSTSTADPNPSAPAIPEVVQRTSASAPGG GTTSGLDGEWLFWRKRWRFPQGTLAGQVLATVGLICNSD

		TCTACAGCCGATCCCAACCCGAGCGCACCCGCCATCCCGGAGGTTGTGCAACGC ACGTCCGCATCTGCCCCTGGTGGAGGTACTACGTCGGGCCTGGATGGCGAGTGG CTGTTCTGGCGGAAGCGTTGGAGATTCCCGCAGGGCACCCTAGCTGGTCAAGTCC TGGCCACCGTGGGCCTCATCTGCAACTCGGATCGTCGCTTCGAGAGTAACACGGG TGAGCTGATCCCGAAGGATACCCCGCTGTCGTACACTCGCATCAAGGACGCCGCC GGGCAGCCTACTACTCTGGTGGTGGCCGCTGACGAGATTCTGGATGTCCAGTACG AGTTCCGCAGCCGGCCCGTAGGAACGGCTGAGGCCAAGTTCGTGATCTCCGGCG TGGAACGCACCTTCCGGCTGATCCCACAGCCTTTTGCGAACCGTGCTAATCTCTC CGGGGAACGCTACATCTTCTACAACACCAACCCCTACATCAACGGCAAGGACGCC TCCGGCGGCAATGTCCGAGACGGTCAGTGGCAGAAGAAATATCCCAAGTACGTGC GCGGCTCCTACAAGGCGCAGATCACGCTGCTGGCCCAGGTCCAGAACGGCAATA TGGCTGGCGGCATCACCGGCACCGAGGAACTCCAGATTTACAATGGACGTAACTA TGTGCTCGATATCAACCCGCCTGTTGTGAAGAACAATACCCAGGAGTTCACCGTGA CCCTGGAGTTTACGGTGGCGAGGGCATAA	RRFESNTGELIPKDTPLSYTRIKDAAGQPTTLVVAADEILDV QYEFRSRPVGTAEAKFVISGVERTFRLIPQPFANRANLSGER YIFYNTNPYINGKDASGGNVRDGQWQKKYPKYVRGSYKAQ ITLLAQVQNGNMAGGITGTEELQIYNGRNYVLDINPPVVKN NTQEFTVTLEFTVARA
PE3	47	ATGGCACTGATCTACGACTTCAACCCAGACCTTGATCCGAAGGCTAAGTCCAAGTT CGTAGGTGCGCGAGGCCGTAGGGACATCAGCGACGTGCTGGACTTCTGCGACGG GGGTGTGGCTATCCAGGACCCGTCGCAGGGCATGATGGTCCGCGTGTGGCGAAC AGAGCTTCGCCAGGACGGGACCTACCTGGGTCACGAGGACGGCTCGAACGAGAT TCGCATCGGCGGAGGTATCGAAGAAGGTATCTCCACGATGTCCCTCGACTTCGAC AGCAACATGAACTACGTGTGTGCTTTCGTACGAGCCGACCGGACTGGTGCAATCT CCTACTTCAACGTGCAGCAGGGCCGCCGGCTCCTCGTGGAGCTTGGGCAGGTTG ACTATGCCAAGGTGGCCCTGGACGACAAACGTCCGGGGGCTACCGCCTGGGCGC AGGTTATCGTGCCCTACACACGCAACGGGAACCTCTACGTCCGCACGCAAAATGA GAACTACACCGAAGAGCACCTGGAGGTGGATACCGGCAAGGTATTCCGGCCTCTG GTGAAATGCGGTATGGGCACCAACCTCCGCTTCCAAGTCCAATTCAGAGGGCACA TGTAA	MALIYDFNPDLDPKAKSKFVGARGRRDISDVLDFCDGGVAI QDPSQGMMVRVWRTELRQDGTYLGHEDGSNEIRIGGGIEE GISTMSLDFDSNMNYVCAFVRADRTGAISYFNVQQGRRLL VELGQVDYAKVALDDKRPGATAWAQVIVPYTRNGNLYVRT QNENYTEEHLEVDTGKVFRPLVKCGMGTNLRFQVQFRGH M

In silico annotation of phages A2 and PE3 are represented in **Table S3** and **Table S4**, respectively. For that, it was used five different platforms: myRAST, BLASTP, PFAM, InterPro and HHpred. The genes that are shaded in the table are those selected for further cloning, expression and functional analysis.

Table S3 – Annotation of phage A2. For each locus_tag, the transcription start and stop position. The corresponding gene product size and putative predicted function based on the best hit and E-value obtained

locus_tag	Minimum (bp)	Maximum (bp)	Length (bp)	Putative Function	Best Species Hit	E-value
phiIBBPAA2_0001	1138	1443	306	hypothetical protein	Pseudomonas phage phiIBB-PAA2	1.0E-67
phiIBBPAA2_0002	1447	1929	483	hypothetical protein	Pseudomonas phage phiIBB-PAA2	2.0E-110
phiIBBPAA2_0003	1987	2220	234	hypothetical protein	Pseudomonas phage phiIBB-PAA2	2.0E-47
phiIBBPAA2_0004	2217	2357	141	hypothetical protein	Pseudomonas phage PSA13	1.0E-23
phiIBBPAA2_0005	2537	2719	183	hypothetical protein	Pseudomonas virus LUZ24	2.0E-33
phiIBBPAA2_0005A	2719	2841	123	hypothetical protein	Pseudomonas phage phiIBB-PAA2	2.0E-18
phiIBBPAA2_0006	2851	3084	234	hypothetical protein	Pseudomonas virus LUZ24	3.0E-48
phiIBBPAA2_0007	3086	3361	276	hypothetical protein	Pseudomonas phage phiIBB-PAA2	3.0E-60
phiIBBPAA2_0008	3372	3527	156	hypothetical protein	Pseudomonas phage PSA13	2.0E-27
phiIBBPAA2_0009	3514	3660	147	hypothetical protein	Klebsiella pneumoniae	2.0E-27
phiIBBPAA2_0010	3669	3914	246	hypothetical protein	Pseudomonas phage phiIBB-PAA2	1.0E-52
phiIBBPAA2_0011	3919	4185	267	hypothetical protein	Pseudomonas phage phiIBB-PAA2	3.0E-58
phiIBBPAA2_0012	4185	4448	264	hypothetical protein	Pseudomonas phage vB_PaeP_C1-14_Or	1.0E-56
phiIBBPAA2_0013	4448	4717	270	hypothetical protein	Pseudomonas phage phiIBB-PAA2	5.0E-55
phiIBBPAA2_0014	4717	5142	426	hypothetical protein	Pseudomonas phage phiIBB-PAA2	4.0E-101

phiIBBPAA2_0015	5268	5495	228	hypothetical protein	Pseudomonas phage phiIBB-PAA2	3.0E-44
phiIBBPAA2_0016	5485	5937	453	hypothetical protein	Klebsiella pneumoniae	2.0E-107
phiIBBPAA2_0017	5944	6273	330	hypothetical protein	Pseudomonas phage phiIBB-PAA2	1.0E-76
phiIBBPAA2_0018	6312	7331	1020	hypothetical protein	Pseudomonas phage phiIBB-PAA2	0.0
phiIBBPAA2_0019	7350	8306	957	hypothetical protein	Pseudomonas phage phiIBB-PAA2	0.0
phiIBBPAA2_0020	8303	9103	801	COOH-NH2 ligase-type 2	Phage phiEco32	5.9E-08
phiIBBPAA2_0021	9096	9665	570	hypothetical protein	Pseudomonas phage phiIBB-PAA2	4.0E-137
phiIBBPAA2_0022	9641	10816	1176	hypothetical protein	Pseudomonas phage phiIBB-PAA2	0.0
phiIBBPAA2_0023	10828	12360	1533	GATase_6 (2×)	Pseudomonas phage phiIBB-PAA2	8.2E-23
phiIBBPAA2_0024	12370	12591	222	hypothetical protein	Pseudomonas phage phiIBB-PAA2	2.0E-44
phiIBBPAA2_0025	12722	13603	882	Putative acetylornithine deacetylase	Pseudomonas phage phiIBB-PAA2	6.1E-20
phiIBBPAA2_0026	13603	14001	399	hypothetical protein	Pseudomonas virus LUZ24	3.0E-92
phiIBBPAA2_0027	14001	14378	378	hypothetical protein	Pseudomonas phage phiIBB-PAA2	5.0E-88
phiIBBPAA2_0028	14379	16088	1710	primase/helicase	Pseudomonas phage phiIBB-PAA2	5.1E-70
phiIBBPAA2_0029	16072	16581	510	DNA polymerase part I	Pseudomonas phage vB_PaeP_C2-10_Ab22	4.0E-121
phiIBBPAA2_0030	16563	16859	297	hypothetical protein	Pseudomonas phage phiIBB-PAA2	2.0E-57
phiIBBPAA2_0031	16895	17128	234	hypothetical protein	Pseudomonas virus Pa223	3.0E-44
phiIBBPAA2_0032	17109	17300	192	hypothetical protein	Pseudomonas phage TL	1.0E-36
phiIBBPAA2_0033	17290	17451	162	hypothetical protein	Pseudomonas phage phiIBB-PAA2	1.0E-28
phiIBBPAA2_0034	17442	17726	285	putative holin	Pseudomonas phage phiIBB-PAA2	2.0E-59

phiIBBPAA2_0035	17797	18306	510	hypothetical protein	Pseudomonas phage phiIBB-PAA2	2.0E-120
phiIBBPAA2_0036	18311	18508	198	hypothetical protein	Pseudomonas phage phiIBB-PAA2	2.0E-38
phiIBBPAA2_0037	18509	20146	1638	DNA polymerase part II	Pseudomonas phage phiIBB-PAA2	6.2E-52
phiIBBPAA2_0037A	20128	20535	408	hypothetical protein	Pseudomonas phage phiIBB-PAA2	3.0E-97
phiIBBPAA2_0038	20605	21159	555	hypothetical protein	Pseudomonas virus LUZ24	3.0E-131
phiIBBPAA2_0039	21137	21640	504	hypothetical protein	Pseudomonas phage phiIBB-PAA2	6.0E-120
phiIBBPAA2_0040	21612	21896	285	hypothetical protein	Pseudomonas phage phiIBB-PAA2	6.0E-61
phiIBBPAA2_0041	21896	22780	885	5'-3' exonuclease	Pseudomonas phage phiIBB-PAA2	1.4E-25
phiIBBPAA2_0042	22755	23741	987	hypothetical protein	Pseudomonas phage phiIBB-PAA2	0.0
phiIBBPAA2_0043	23927	24688	762	hypothetical protein	Pseudomonas aeruginosa	2.8E-15
phiIBBPAA2_0044	24685	24903	219	hypothetical protein	Pseudomonas virus LUZ24	2.0E-44
phiIBBPAA2_0045	24907	25116	210	hypothetical protein	Pseudomonas phage SaPL	1.0E-41
phiIBBPAA2_0045A	25103	25309	207	hypothetical protein	Pseudomonas phage phiIBB-PAA2]	4.0E-38
phiIBBPAA2_0046	25516	25872	357	hypothetical protein	Pseudomonas phage phiIBB-PAA2	5.0E-80
phiIBBPAA2_0047	25887	26774	888	virion protein	Pseudomonas phage phiIBB-PAA2	0.0
phiIBBPAA2_0048	26786	29953	3168	virion protein	Pseudomonas phage phiIBB-PAA2	0.0
phiIBBPAA2_0049	30104	31618	1515	virion protein	Pseudomonas phage phiIBB-PAA2	0.0
phiIBBPAA2_0050	31623	32003	381	virion protein	Pseudomonas phage phiIBB-PAA2	3.0E-79
phiIBBPAA2_0051	32003	32944	942	hypothetical protein	Pseudomonas phage phiIBB-PAA2	0.0
phiIBBPAA2_0052	32925	33359	435	hypothetical protein	Pseudomonas phage PSA16	4.0E-102

phiIBBPAA2_0053	33356	34045	690	RBP	Listeria	3. 0E-02
phiIBBPAA2_0054	34042	35583	1542	viral protein	Enterobacteria phage T7	6.7E-06
phiIBBPAA2_0055	35592	36239	648	RB domain of short TFP gp12	Bizionia argentinensis JUB59	79
phiIBBPAA2_0056	36229	36477	249	hypothetical protein	Pseudomonas virus Pa223	1.0E-49
phiIBBPAA2_0057	36461	36652	192	hypothetical protein	Pseudomonas virus LUZ24	1.0E-34
phiIBBPAA2_0058	36663	37289	627	virion protein	Pseudomonas virus LUZ24	1.0E-151
phiIBBPAA2_0059	37293	37613	321	hypothetical protein	Pseudomonas virus LUZ24	5.0E-72
phiIBBPAA2_0060	37662	38615	954	major head protein	Microcystis phage Mic1	2.0E-101
phiIBBPAA2_0061	38634	39626	993	scaffolding protein	Pseudomonas aeruginosa	0.0
phiIBBPAA2_0062	39626	39868	243	hypothetical protein	Pseudomonas aeruginosa	4.0E-51
phiIBBPAA2_0063	39871	41991	2121	portal protein	Pseudomonas phage phiIBB-PAA2	2.2E-40
phiIBBPAA2_0064	41991	43439	1449	terminase large subunit	Pseudomonas virus LUZ24	5.0E-47
phiIBBPAA2_0065	43439	43837	399	lysozyme	Pseudomonas phage TL	2.0E-89
phiIBBPAA2_0066	43869	44327	459	hypothetical protein	Pseudomonas phage phiIBB-PAA2	5.0E-107

Table S4 - Annotation of phage PE3. For each locus_tag, the transcription start and stop position. The corresponding gene product size and putative predicted function based on the best hit and E-value obtained

locus_tag	Minimum (bp)	Maximum (bp)	Length (bp)	Putative function	Best Species Hit	E-value
vBPaePPE3_001	1776	2060	285	hypothetical protein	Pseudomonas phage phiKMV	4.0E-62
vBPaePPE3_002	2060	2287	228	hypothetical protein	Pseudomonas phage phiKMV	5.0E-46

vBPaePPE3_003	2298	2837	540	hypothetical protein	Pseudomonas phage LUZ19	5.0E-128
vBPaePPE3_004	2834	3004	171	hypothetical protein	Pseudomonas phage vB_PaeP_130_113	1.0E-32
vBPaePPE3_005	3007	3126	120	hypothetical protein	Pseudomonas phage vB_PaeP_PE3	7.0E-18
vBPaePPE3_006	3205	3573	369	hypothetical protein	Pseudomonas phage phiKMV	4.0E-85
vBPaePPE3_007	3560	3787	228	hypothetical protein	Pseudomonas phage phiKMV	7.0E-49
vBPaePPE3_008	3784	3969	186	hypothetical protein	Pseudomonas phage vB_PaeP_PE3	3.0E-34
vBPaePPE3_009	3966	4139	174	hypothetical protein	Pseudomonas aeruginosa	3.0E-34
vBPaePPE3_010	4139	4420	282	hypothetical protein	Pseudomonas aeruginosa	2.0E-59
vBPaePPE3_011	4420	4680	261	hypothetical protein	Pseudomonas aeruginosa	4.0E-55
vBPaePPE3_012	4682	4969	288	hypothetical protein	Pseudomonas phage vB_PaeP_PE3	2.0E-63
vBPaePPE3_013	5048	5464	417	hypothetical protein	Pseudomonas phage vB_PaeP_PE3	1.0E-92
vBPaePPE3_014	5533	5892	360	hypothetical protein	Pseudomonas phage phiKMV	2.0E-78
vBPaePPE3_015	5895	6704	810	DNA-binding protein	Pseudomonas phage vB_PaeP_PE3	0.0
vBPaePPE3_016	6784	7203	420	hypothetical protein	Pseudomonas phage vB_PaeP_PE3	7.0E-98
vBPaePPE3_017	6974	7516	543	hypothetical protein	Pseudomonas phage vB_PaeP_PE3	3.0E-129
vBPaePPE3_018	7526	7729	204	hypothetical protein	Pseudomonas phage PT5	3.0E-41
vBPaePPE3_019	7702	8526	825	putative DNA primase	Aquifex aeolicus	1.3E-22
vBPaePPE3_020	8495	9763	1269	DNA helicase	Bacillus phage SPP1	1.5E-39
vBPaePPE3_021	9753	10370	618	putative nucleotidyl transferase	Pseudomonas phage vB_PaeP_PE3	2.0E-148
vBPaePPE3_022	10370	11317	948	DNA ligase	Pseudomonas phage vB_PaeP_PE3	1.5E-37

vBPaePPE3_023	11320	11649	330	hypothetical protein	Pseudomonas phage vB_PaeP_PE3	2.0E-74
vBPaePPE3_024	11646	14069	2424	DNA polymerase I	Plasmodium falciparum	6.0E-64
vBPaePPE3_025	14066	14377	312	hypothetical protein	Pseudomonas phage LKD16	2.0E-69
vBPaePPE3_026	14432	15481	1050	hypothetical protein	Pseudomonas phage MPK7	0.0
vBPaePPE3_027	15481	16422	942	5'-3' exonuclease	Mycobacterium smegmatis	4.3E-30
vBPaePPE3_028	16412	16852	441	putative DNA endonuclease VII	Pseudomonas phage MPK6	5.0E-105
vBPaePPE3_029	16849	17895	1047	DNA polymerase	Pyrobaculum calidifontis	2.7E-10
vBPaePPE3_030	17905	18267	363	hypothetical protein	Pseudomonas phage vB_PaeP_PE3	1.0E-80
vBPaePPE3_031	18260	18610	351	hypothetical protein	Pseudomonas phage vB_PaeP_PE3	4.0E-78
vBPaePPE3_032	18619	21066	2448	putative DNA-dependent RNA polymerase	Enterobacteria phage T7	6.0E-152
vBPaePPE3_033	21240	21491	252	hypothetical protein	Pseudomonas phage LUZ19	1.0E-52
vBPaePPE3_034	21491	21964	474	putative acetyltransferase	Pseudomonas phage vB_PaeP_PE3	5.0E-114
vBPaePPE3_035	21909	22205	297	putative structural protein	Pseudomonas phage vB_PaeP_PE3]	4.0E-61
vBPaePPE3_036	22217	23749	1533	putative head-tail connector protein	Enterobacteria phage T7	5.6E-91
vBPaePPE3_037	23753	24721	969	scaffolding protein	Pseudomonas phage vB_PaeP_PE3	0.0
vBPaePPE3_038	24774	25781	1008	capsid protein	Pseudomonas phage phiKMV	0.0
vBPaePPE3_039	25878	26432	555	tail tubular protein A	Pseudomonas phage LUZ19	8.0E-132
vBPaePPE3_040	26435	28915	2481	tail tubular protein B	Enterobacteria phage T7	8.3E-110
vBPaePPE3_041	28915	29460	546	putative internal virion protein A	Pseudomonas phage phiKMV	2.0E-124

vBPaePPE3_042	29460	32156	2697	internal virion protein	Pseudomonas phage vB_PaeP_PE3	0.0
vBPaePPE3_043	32160	36173	4014	internal virion protein	Pseudomonas phage vB_PaeP_PE3	0.0
vBPaePPE3_044	36175	36930	756	putative tail fiber protein	Enterobacteria phage T7	4.6E-11
vBPaePPE3_045	36930	37388	459	tail fiber protein	Pseudomonas phage LUZ19	7.0E-106
vBPaePPE3_046	37381	38286	906	tail fiber protein	Pseudomonas phage vB_PaeP_PE3	0.0
vBPaePPE3_047	38290	38895	606	tail fiber protein	Pseudomonas phage LUZ19	9.0E-148
vBPaePPE3_048	38895	39200	306	hypothetical protein	Pseudomonas phage vB_PaeP_PAO1_1-15pyo	1.0E-68
vBPaePPE3_049	39210	41015	1806	terminase large subunit	Pseudomonas phage vB_PaeP_PE3	1.4E-32
vBPaePPE3_050	41012	41212	201	hypothetical protein	Pseudomonas phage phiKMV	2.0E-38
vBPaePPE3_051	41209	41691	483	endolysin	Pseudomonas phage vB_PaeP_PE3	1.0E-114
vBPaePPE3_052	41649	41978	330	hypothetical protein	Pseudomonas phage DL62	4.0E-72
vBPaePPE3_053	42130	42480	351	minor structural protein	Pseudomonas phage vB_PaeP_PE3	3.0E-72
vBPaePPE3_054	42499	42744	246	particle protein	Pseudomonas phage vB_PaeP_PE3	3.0E-49
vBPaePPE3_055	42753	42968	216	hypothetical protein	Pseudomonas phage LUZ19	3.0E-42